Doctor of Philosophy

Studies on mitochondrial DNA mutations in induced pluripotent stem cells and their differentiated pancreatic cells with type 2 diabetes

제 2형 당뇨 환자 유래 유도만능줄기세포와 그로부터 분화된 췌장세포의 미토콘드리아 DNA 돌연변이에 관한 연구

The Graduate School

of the University of Ulsan

Department of Medical science

Seongjun So

Studies on mitochondrial DNA mutations in induced pluripotent stem cells and their differentiated pancreatic cells with type 2 diabetes

Supervisor Song-Cheol Kim

A Dissertation

Submitted to

the Graduate School of the University of Ulsan

In partial Fulfilment of the Requirements

for the Degree of

Doctor of Philosophy

By

Seongjun So

Department of Medical science

University of Ulsan, Korea

August 2022

This certifies that the dissertation

of Seongjun So is approved.

Committee Chair Dr. In-Kyong Shim

Committee Member Dr. Song-Cheol Kim

Committee Member Dr. Eunju Kang

Committee Member Dr. Hyun-Ju Yoo

Committee Member Dr. Deokhoon Kim

Department of Medical science

University of Ulsan, Korea

August 2022

감사의 글

박사 학위를 마무리 하면서 부족함과 아쉬움도 많지만 그보다는 너무나 소중한 것을 많이 얻을 수 있었던 대학원 생활이었습니다. 돌이켜보면 학업의 시작부터 논문의 완성까지 너무나 많은 고마운 분들의 도움으로 이 자리에 올수 있었다고 생각됩니다.

항상 세심한 지도와 많은 격려로 제가 나아갈 수 있도록 이끌어 주신 강은주 교수님께 진심으로 감사드립니다. 부족한 저에 대한 교수님의 깊은 믿음과 가르침이 없었다면 이 자리까지 올 수 없었을 것입니다. 또한 저를 믿어주시고 이렇게 무사히 학위를 마칠 수 있도록 도움을 주신 김송철 교수님께 깊은 감사의 말씀을 전합니다. 학위논문 심사 기간 동안 피가 되고 살이 되는 많은 조언과 지도를 해주신 심인경 교수님, 김덕훈 교수님, 그리고 유현주 교수님께도 감사드립니다.

연구실 생활 동안 많은 조언과 도움을 주신 이연미 박사님과 실험 과정에서 마치 자신의 일처럼 도와주고 많은 힘이 되어준 한종석 학우, 힘들때마다 흔쾌히 힘을 보태주었던 최지완, 김빛나라, 손형빈, 진채연 학우들께도 감사함을 전합니다. 앞으로 하고자 하는 분야에서 최고가 될 수 있기를 기원하겠습니다. 또 일일히 언급할 순 없지만 그 외에도 많은 힘이 되어준 친지분들께 감사드립니다. 힘들때마다 정말 큰 힘이 되었습니다.

마지막으로 오늘이 있기까지 늘 저를 믿어주시고 사랑으로 이끌어주신 저희 부모님께 깊은 사랑과 감사함을 전합니다. 온 마음을 다해 길러주신 그 은혜를 다 갚을 순 없겠지만 평생 갚도록 노력하겠습니다.

지금이 오기까지 도움을 주셨던 모든 분들게 다시 한번 감사하다는 말씀을 드리며 믿음에 어긋나지 않는 훌륭한 연구자가 되도록 더욱더 노력하겠습니다. 감사합니다.

국문 요약

당뇨병은 인슐린 생산 감소 또는 신체의 인슐린 저항성로 인해 혈당 수치가 비정상적으로 상승하는 심각한 질병이다. 최근 몇 년 동안 전 세계적으로 당뇨병의 유병률이 증가했으며 이는 높은 사망률의 원인 중 하나이다. 현재 당뇨병에 대한 질병 모델링 또는 치료제로서 인간 유도 만능 줄기 세포(iPSC)를 이용한 많은 연구가 수행되고 있다. 그러나 당뇨환자 유래의 iPSC의 미토콘드리아 게놈(mtDNA)의 돌연변이가 어떤 경향으로 나타나는지는 아직 연구되지 않았고 이러한 mtDNA 돌연변이가 인슐린을 분비하는 췌장 베타 세포로의 분화 및 기능에 어떠한 영향을 미치는지는 정확히 밝혀지지 않았다. 우리는 3명의 2형 당뇨병(T2D) 환자와 당뇨병이 아닌 환자 3명에서 섬유아세포, 혈액 세포 및 췌장 세포를 수집하고 iPSC를 수립하여 mtDNA 돌연변이를 분석하였다. T2D-iPSCs에서 mtDNA의 돌연변이는 조직이나 환자 사이에서 특정한 경향 없이 무작위로 발견되었으며 환자간 공유 돌연변이는 발견되지 않았다. T2D-iPSC 클론 중 62% (21/34)는 한 개 이상의 mtDNA 돌연변이를 갖고 있었으며, 그 중 37%는 돌연변이 수준이 100%인 homoplasmy였고 비당뇨병에서 homoplasmic mtDNA 돌연변이는 8%에 불과했다. 또한, 높은 heteroplasmic mtDNA 돌연변이를 가진 클론은 정상 유전형에 비해 낮은 mtDNA 복제 수를 보였다.

다음으로 우리는 정상 유전형을 갖는 iPSC와 돌연변이를 갖는 iPSC를 선택해 췌장 세포로 분화하여 mtDNA 돌연변이가 췌장 분화에 미치는 영향을 조사하였다. 돌연변이 iPSC로부터 분화한 췌장 전구 세포의 췌장 발달 관련 유전자 및 단백질 발현은 정상 유전형에 비해 유의하게 낮았다. 또한, mtDNA 돌연변이를 갖는 분화 췌장세포에서 미토콘드리

아 호흡과 해당과정 및 TCA 회로 관련 대사 산물 수준이 정상 유전형에 비해 유의하게 낮았다. 돌연변이 세포주는 인슐린 분비가 정상에 비해 감소하였으며 글루코스에 반응하여 인슐린 분비가 증가하지 않았다. 이러한 결과는 당뇨병 환자의 iPSC를 이용한 질병 모델링 또는 자가 세포 치료를 위한 췌장 세포 분화 이전에 mtDNA 돌연변이를 스크리닝하는 것이 필수적임을 시사한다.

Abstract

Diabetes mellitus (DM) is a serious disease in which blood sugar levels rise abnormally because of failed insulin production or decreased insulin sensitivity. In recent years, the prevalence of DM has increased worldwide, which is one of the causes of high mortality. Many studies have been conducted using human-induced pluripotent stem cells (iPSCs) as a disease modeling and potential treatment for DM. However, whether mitochondria genome (mtDNA) abnormalities in iPSCs affected β-cell differentiation and function has not been investigated. First, we established a more effective and xeno-free pluripotent stem cell culture using fasudil, which is safe and cost-effective, instead of Y-27632, a rho-associated protein kinase (ROCK) inhibitor commonly used for pluripotent stem cell culture. Then, we collected iPSCs from fibroblasts, PBMCs, and pancreatic cells of three type 2 DM (T2D) patients and three patients with non-diabetes counterparts and analyzed mtDNA mutations. The mtDNA mutations in T2D-iPSCs were detected randomly without any tendency among tissues or patients, and there were no shared mutations. The 62% (21/34) of T2D-iPSC lines harbored various mtDNA mutations, of which 37% were homoplasmy at 100% mutation level compared to only 8% in non-diabetes. In addition, clones with high heteroplasmic mtDNA mutations had low mtDNA copy numbers. We selected iPSC lines that were either wild-type or mutant mtDNA and differentiated into pancreatic cells. The expression of mRNA and protein of pancreatic development-related genes was significantly lower with mtDNA mutations compared with that of the wild type. In addition, the oxygen consumption rates and metabolite levels were significantly lower in the mtDNA mutant cells. Furthermore, the mutant cell lines exhibited decreased production of insulin and reduced secretion of insulin in response to glucose. Overall, the results suggest that screening for mtDNA mutations in iPSCs from type 2 DM patients is an essential step in pancreatic cell differentiation for disease modeling or autologous cell therapy.

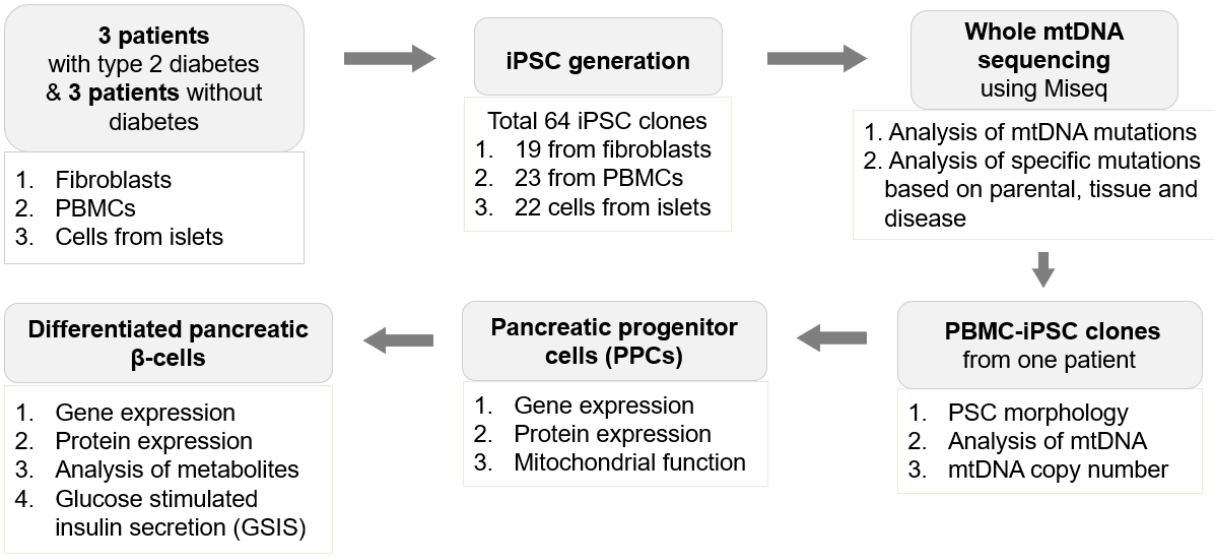

Experimental design of the study. Fibroblasts, PBMCs, and pancreatic cells were isolated from 3 patients with type 2 diabetes and 3 patients without diabetes, and iPSCs were induced. The iPSC clones were analyzed for mtDNA mutations, and PBMC-derived iPSCs from one patient were selected. These iPSC clones were analyzed for mtDNA copy number and differentiated into pancreatic progenitor cells and the expression of differentiation markers. Finally, wild and mutant clones were selected and differentiated into pancreatic β-cells. Then, the effect of mtDNA mutation on the expression of differentiation markers, metabolism, and glucose-stimulated insulin secretion in β-cell was investigated.

Contents

List of Tables

List of Figures

Abbreviations

PSC: Pluripotent stem cell

ESC: Embryonic stem cell

iPSC: Induced pluripotent stem cell

ROCK: Rho-associated kinase

DNA: DeoxyriboNucleic Acid

mtDNA: Mitochondrial DNA

DM: Diabetes mellitus

T2D: Type 2 diabetes

PBMC: Peripheral blood mononuclear cell

OCT4: Octamer-binding transcription factor 4

SOX2: Sex determining region Y-box 2

KLF4: Kruppel-like factor 4

ATP: Adenosine triphosphate

cAMP: Cyclic adenosine monophosphate

NADPH: Nicotinamide adenine dinucleotide phosphate

FBS: Fetal bovine serum

PCR: Polymerase chain reaction

cDNA: complementary DNA

PDX1: Pancreatic and duodenal homeobox 1

PBS: Phosphate buffered saline

OCR: Oxygen consumption rate

NGN3: Neurogenin-3

NKX6.1: NK6 Homeobox 1

CNV: Copy number variation

GLC: Glucose; G6P, glucose-6-phosphate

F6P: Fruc-tose-6-phosphate

CIT: Citrate

ISO CIT: Iso-citrate

AKG: Alpha-ketoglutarate

SUC: Succinate

MAL: Malate

NAD: Nicotinamide adenine dinucleotide

OAA: Oxaloacetate

ELISA: Enzyme-linked immunosorbent assay

GSIS: Glucose-stimulated insulin secretion

Chapter I.

General introduction

1. Diabetes mellitus

Diabetes is widely recognized as a metabolic disease that causes several complications due to an increase in blood sugar levels in the body. It is known that diabetes can be caused by several factors such as autoimmune, metabolic disorders, obesity, and genetic factors (1). Prolonged exposure to high blood sugar can affect the kidneys, retina, or peripheral nervous system, resulting in complications. According to the International Diabetes Federation, approximately 416 million people worldwide were diagnosed with diabetes in 2015, and this number is expected to increase further in the future. Diabetes is divided into type 1 diabetes and type 2 diabetes. Type 1 diabetes is caused by damage to the β-cells because of an autoimmune response to the islet cells in the pancreas, resulting in the inability to produce insulin. On the other hand, type 2 diabetes is caused by various factors such as genetic factors related to insulin resistance and obesity, overeating, lack of exercise and stress, and aging (2). Exogenous insulin supplementation can be a diabetes treatment, but it is difficult to accurately control blood sugar levels physiologically. Transplanting islet tissue or the entire pancreas can be an effective treatment for type 1 diabetes and end-stage type 2 diabetes, but there are several problems such as donor shortage and the potential risk of tissue rejection (3). To solve this problem, many researchers have been conducting studies to applicate pancreatic β-cells differentiated from iPSCs as autologous cell therapy (4-6).

2. Induced pluripotent stem cells

Human-induced pluripotent stem cells (iPSCs) artificially created pluripotent stem cells, first reported in 2007 by Dr. Yamanaka's team using human fibroblast (7). iPSCs can be generated by the transduction of four Yamanaka factors (*OCT4, SOX, KLF4,* and *c-MYC*) into somatic cells. Similar to embryonic stem cells, iPSCs have pluripotency to differentiate into three-germ layer tissues and self-renewal properties. Because of these properties, iPSCs have the potential to be an important source of almost all cell types for basic research, drug development, and autologous cell therapy. However, dissociation of hPSCs for processes common in stem cell research processes, such as passage, expansion, cryopreservation, gene transfer, differentiation induction, and cell sorting, causes massive apoptosis (8). Thus, hPSCs were originally cultured using the feeder layer technique to increase their survival and maintain pluripotency (9). Mouse embryonic fibroblasts (MEFs) are the most commonly used feeder cells in research, but they are not suitable for xeno-free culture for clinical research due to problems with cell contamination. So, many researchers have used a selective Rho-associated kinase (ROCK) inhibitor, Y-27632, which has been reported to reduce dissociation-induced apoptosis and increase

cloning efficiency for the effective xeno-free culture of iPSCs (10). There are several ROCK inhibitors available on the market, including RKI-1447, GSK429286A, and fasudil. In particular, fasudil (HA-1077, 5-[1,4-diazepan-1-ylsulfonyl] isoquinoline) is much easier to synthesize and more cost-effective than Y-27632. Fasudil is also approved for clinical use and is already used in Japan and China for the prevention of cerebral vasospasm after subarachnoid hemorrhage. Fasudil has been also reported to increase the growth of PSC effectively and safely (11).

3. Mitochondrial DNA

Mitochondria are cytoplasmic organelles that generate the majority of cellular energy in the form of adenosine triphosphate (ATP) by oxidative phosphorylation (OXPHOS) in all nucleated cells. Mitochondria also play an essential role in processes such as the TCA cycle, β-oxidation of fatty acids, and calcium processing, and also play a very important role in regulating apoptosis and the cell cycle (12). Mitochondria are the only organelles in the cell where DNA exists outside of chromosomes, and various proteins in mitochondria are under the control of both nuclear DNA and the mitochondrial genome (13). Human mitochondrial DNA (mtDNA) is a 16,569 bp double-stranded circular molecule, and multiple copies of mtDNA are present in each mitochondrion. Human mitochondrial DNA encodes 13 proteins that form the mitochondrial respiratory chain, along with 22 transfer RNAs and 2 ribosomal RNAs required for protein synthesis (14). Because mtDNA is vulnerable to stress-induced damage due to its lack of protective histone protein and limited DNA repair mechanism, the mutation rate is higher than that of genomic DNA (15). mtDNA mutations are an important cause of genetic disorders (13). For example tRNALeu(UUR) mt3243A >G mutation is known to be a highly lethal mutation that can cause diabetes, neurodegenerative diseases, or fatal childhood diseases (16, 17). In addition, levels of somatic mtDNA mutations tend to increase with age (18, 19). It has been reported that somatic mtDNA mutations and mitochondrial respiratory chain dysfunction can lead to various phenotype-related diseases (20). Reportedly, individual iPSC clones, each derived from a single cell, may have various mtDNA mutations causing functional abnormalities, even if they have the identical genotype of genomic DNA. These mutations are already present in parental cells, not generated during reprogramming, and can affect cell function independently of genomic DNA (19). Therefore, even if the genotype of the genomic DNA is the same, the difference in cell function may vary depending on the mtDNA mutations of each iPSC clone.

Chapter II.

Study of efficient xeno-free culturing of pluripotent stem cells

1. Abstract

Poor survival of human pluripotent stem cells (hPSCs) following freezing, thawing, or passaging hinders the maintenance and differentiation of stem cells. Rho-associated kinases (ROCKs) play a crucial role in hPSC survival. To date, a typical ROCK inhibitor, Y-27632, has been the primary agent used in hPSC research. Before we enter into full-scale iPSC research in diabetic patients, we investigated that another ROCK inhibitor, fasudil, can be used as an alternative and is cheaper than Y-27632. It increased hPSC growth following thawing and passaging, like Y-27632, and did not affect pluripotency, differentiation ability, and chromosome integrity. It was also useful for single-cell passaging of hPSCs and during aggregation. These findings suggest that fasudil can replace Y-27632 for use in pluripotent stem cell research.

2. Introduction

Human pluripotent stem cells (hPSCs), such as embryonic stem cells (hESCs) and induced pluripotent stem cells (hiPSCs), are valuable research tools in the fields of developmental biology, disease modeling, drug screening, and regenerative medicine (21-23). However, hPSCs are difficult to culture because of their poor survival, especially when they are detached from surfaces or dissociated for freezing (24-26). Hence hPSCs were initially cultured on feeder layers to increase their survival and maintain pluripotency.

Mouse embryonic fibroblasts (MEFs) are the most commonly used feeder cells in research but may have limited efficacy with human cells due to xenogeneic contamination (26, 27). Another disadvantage of MEFs is that the use of any feeder layer itself leads to batch- or lab-dependent variation; additionally, feeder layers increase workload, which subsequently limits large-scale hPSC culture (28, 29). To overcome these problems, additional methods have been introduced, such as culturing hPSCs in suspension with microcarriers or on synthetic polymers (30). As a result, feeder-free hPSC cultures became possible when hPSCs were grown on an extracellular matrix with specialized small molecules and growth factors (30, 31).

In 2007, Y-27632 ([1R,4r]-4-[(R)-1-aminoethyl]-N-[pyridin-4-yl] cyclohexane carboxamide), the first small molecule to inhibit the Rho-associated kinase (ROCK) pathway, was reported to increase the survival and growth of PSCs; since then, it has been used extensively in stem cell research (10). It has also been used to encourage PSC differentiation in endodermal lineage cells (32) and insulin-producing cells (33), and for promoting the maturation or maintenance of differentiated cells (34-36). The ROCK signal activates the phospho-myosin light chain (pMLC), which contracts intracellular actomyosin and is known to induce apoptosis in dissociated cells (37).

Recently, many researchers have used ROCK inhibitors as essential small molecules for PSC culture. Since Y-27632 was developed and put into use, researchers have primarily resorted to this ROCK inhibitor for PSCs. However, the synthesis of Y-27632 consists of seven steps, and the yield is only 45%, which tends to increase its cost (38). There are several ROCK inhibitors available on the market, including RKI-1447, GSK429286A, H-1152, SLx-2119, TC-S 7001, and fasudil. In particular, fasudil (HA-1077, 5-[1,4-diazepan-1-ylsulfonyl] isoquinoline) is approved for clinical use and is already used in Japan and China for the prevention of cerebral vasospasm after subarachnoid hemorrhage (39). Also, it is synthesized in one step and has a higher yield than Y-27632 (73.1% vs. 45% in Y-27632) (40). To date, however, fasudil has only been used in PSC culture as a control group, but it

has not been clearly characterized for use with hPSCs following long-term culture (10).

In the part II study, we tried to establish an efficient xeno-free PSC culture method prior to further iPSC research. We compared the effectiveness of fasudil and Y-27632 during long-term xeno-free growth and maintenance of hPSCs in conditions of freezing, thawing, and splitting. Fasudil also proved to be useful for inducing 3D differentiation of PSCs.

3. Materials and Methods

1) Ethics and governance

Informed consent was obtained from participants for the use of human samples and use was approved by the institutional review board (IRB: 2017-0260 and 2019-0117) of Asan Medical Center. Experiments on live vertebrates were performed in compliance with the regulations of the Asan Institute for Life Sciences and were approved by the Asan Institutional Animal Care and Use Committee (IACUC: 2018-12-269). All experiments were performed according to relevant guidelines and regulations.

2) Cell culture

Three hESC lines and four hiPSC lines were maintained, based on the hPSC research guidelines of the Stem Cell Center, Asan Medical Center (Seoul, Republic of Korea). The hPSCs were cultured on vitronectin-coated (5 μg/ml; Life Technologies, Grand Island, NY, USA) culture plates in Essential 8 medium (Life Technologies) at 37°C, 5% CO_2. The cultures were passaged every week in clusters by chemically dissociating the PSCs using a lab-made reagent (0.4% sodium citrate, S4641, Sigma-Aldrich, St. Louis, MO, USA) or commercial reagent (Gentle Cell Dissociation Reagent, Stem Cell Technologies, Vancouver, BC, Canada). Dissociation using a lab-made reagent was carried out as described previously (41), and for comparison with a lab-made reagent, the commercial reagent was used according to the manufacturer's instructions. The hPSC clusters were transferred onto prepared vitronectin-coated culture plates supplemented with fasudil (10 uM; Adooq, Irvine, CA, USA) or Y-27632 (10 uM; Sigma-Aldrich).

3) Cell counting

To examine cell growth, sub-confluent cells were dissociated into clumps using a lab-made reagent (sodium citrate) or a commercial reagent. The cell clumps were dissociated into single cells with 0.25% trypsin-EDTA for single-cell counting. These cells were not used for further culture.

4) Living and apoptotic cells

Apoptosis analysis was carried out using a Dead Cell Apoptosis Kit with Annexin V Alexa Fluor 488 & Propidium Iodide (Invitrogen). After staining with Annexin V/PI, floating cells were collected and retained and the attached, Annexin V/PI-stained cells were further counted using a FACS (Canto II, BD Biosciences).

5) Cell proliferation analysis

To determine proliferation, hPSCs were collected and fixed with 10% neutral buffered formalin (BBC Biochemical, Mount Vernon, WA) for 30 minutes at room temperature on the third day after the split. Fixed cells were washed twice with phosphate buffered saline (PBS, Hyclone, Chicago, IL, USA) and permeabilized with 0.05% Triton X-100 in 0.01 M sodium citrate for 30 minutes at room temperature. Ki-67 (Abcam, Cambridge, UK) primary antibody was diluted at 1:200 in PBS containing 10% fetal bovine serum (FBS, Life Technologies) and refrigerated overnight. Thereafter the cells were washed three times with PBS and incubated for 1 hour in the refrigerator with Goat Anti-Rabbit IgG H&L (1:500, Alexa Fluor 555, Abcam) and counted using a FACS (Canto II, BD Biosciences). The FACS data were analyzed with FlowJo xV.0.7 software (Tree Star, Ashland, OR).

6) Quantitative polymerase chain reaction (qPCR)

Total RNAs of hPSCs cultured in the presence of fasudil or Y-27632 were isolated using RNeasy Mini Kits (Qiagen, Valencia, CA, USA), and reverse transcription was performed with cDNA synthesis kits (PCR Biosystems, London, UK). The results were confirmed using a conventional real-time polymerase chain reaction (PCR) analysis. Quantitative reverse transcriptase PCR (RT-qPCR) was then performed using the relevant gene-specific primers, Power SYBR Green PCR Master Mix, and a QuantStudio 6 Flex Real-Time PCR System (Applied Biosystems, Foster City, CA, USA).

7) Immunocytochemistry

Fasudil-treated hPSCs were seeded onto vitronectin-coated plates. Five days after plating, hPSCs were fixed in 10% neutral buffered formalin overnight in a refrigerator (2-8°C), washed twice with PBS, and permeabilized with 0.05% Triton X-100 in 0.01 M sodium citrate for 30 minutes at room temperature if required. Primary antibodies were diluted from 1:100 to 1:500 in PBS containing 10% FBS and incubated overnight in the refrigerator. The primary antibodies, TRA-1-60, SSEA4, and Oct4 (1:100, Stemgent, Cambridge, MA, USA), were used for pluripotency analysis. After incubation with primary antibodies, cells were washed three times with PBS and incubated for 1 hour at room temperature with secondary antibodies. The secondary antibodies were Goat Anti-Mouse IgG H&L (1:1000, Alexa Fluor 488, Abcam), Goat Anti-Rabbit IgG H&L (1:500, Alexa Fluor 555, Abcam), and Goat Anti-Rabbit IgG H&L (1:200, Alexa Fluor 647, Abcam). Samples were imaged and captured using a Carl Zeiss inverted microscope with an AxioCam MRc Rev 3 digital camera (Zeiss, Oberkochen, Germany; Confocal Imaging Core Laboratory, ASAN Institute for Life Sciences, Seoul, Republic of Korea). The expression

population was counted using a FACS (Canto II, BD Biosciences). The FACS data were analyzed with FlowJo xV.0.7 software (Tree Star, Ashland, OR).

8) Teratoma formation

Teratoma formation experiments were performed by injecting hPSCs (maintained in the presence of fasudil for three months and detached from vitronectin-coated plates as cell clumps containing fasudil) into the femoral region of 7-week-old NOD-SCID Gamma mice (NSG, The Jackson Laboratory, Bar Harbor, ME) using a 1 ml syringe (Korea Vaccine Co., Seoul, Republic of Korea). Mice with tumors were euthanized, and teratomas were isolated, sectioned, stained with hematoxylin and eosin (H&E), and histologically characterized for the presence of representative tissues.

9) Karyotyping

Karyotyping was carried out on hPSC lines (hES1, hES2, hES3, hiPS1, and hiPS2) maintained in the presence of 10 μM fasudil over three months by standard G banding at the Medical Genetic Center, Asan Medical Center (Seoul, Republic of Korea).

10) Serum-free 3D PSC aggregation

Aggregated cells were cultured as described previously with minor modifications (10). Dissociated hPSCs (prepared as above; 1.2×10^6 cells/ml) were seeded onto a StemFIT 3D culture dish (MicroFIT, Republic of Korea) and cultured in DMEM/F12 (Life Technologies) supplemented with 20% Knockout Serum Replacement (KSR, Life Technologies), 2 mM glutamine (Life Technologies), 0.1 mM nonessential amino acids (Life Technologies), 0.1 mM 2-mercaptoethanol (Sigma-Aldrich), 100 U/ml penicillin, and 100 mg/ml streptomycin (GE Life Science, Chicago, IL, USA). 10 μM ROCK inhibitor (Y-27632 or fasudil) was added to the culture medium for 24 hours and cultured for six days in the StemFIT 3D culture dishes. The number and size of aggregates were analyzed using the software ImageJ (Wayne Rasband, National Institutes of Health, Bethesda, MD).

11) Single-cell colony-forming assay

Accutase (StemCell Technologies) was used to dissociate hPSCs into single cells, which were then plated at 5×10^3 cells/cm^2 on plates coated with vitronectin in Essential 8 medium. The medium was changed every day and cells were counted after 6 days.

12) Statistical analysis

Statistical comparisons between two groups were made using Student's two-tailed t-test or two-tailed paired t-test. One-way ANOVA with Tukey post hoc analysis using Prism 5 software (GraphPad, San Diego, CA) was used when more than two groups were compared. Data are expressed as mean ± standard deviation (SD).

4. Results and Conclusions

1) Comparable growth of PSCs supplemented with fasudil and Y-27632

To determine the effectiveness of fasudil in PSC culture, we compared the fasudil and Y-27632-mediated hPSC growth of five lines of hPSCs under feeder-free and defined culture conditions. ALP staining was carried out on hPSCs (hES3 and hiPS2) cultured with or without ROCK inhibitors to examine their growth. hPSC colony formation was similar for fasudil and Y-27632, while both groups exhibited higher rates of colony formation than the untreated control (Figure 1A).

Next, we compared the fasudil- and Y-27632-mediated growth of five lines of hPSCs under feeder-free and defined culture conditions. Passaging was performed by an enzyme-free method, part of a commercial and laboratory protocol (41). We evaluated cell growth by the fold increase of cell number. When hPSCs were dissociated and seeded without a ROCK inhibitor, they increased 4 to 39-fold depending on the cell line, whereas, in fasudil, the fold increases were 10 to 89-fold, similar to the Y-27632 culture ($p < 0.05$) (Figure 1B and 1C). The ROCK inhibitors did not affect the growth of hES1.

To understand the mechanisms of PSC growth, we first measured live and apoptotic cell populations using Annexin V and PI. The hES3 and hiPS2 were seeded, then live and apoptotic cell populations were examined 24 hours later (Figure 1D). Both the fasudil- and Y-27632- treated groups had lower apoptotic cell populations than the non-treated controls (34 or 34 % vs. 69% for hES3 and 42 or 41% vs. 59% for hiPS2, $p < 0.05$. We also examined Ki-67 protein expression. Since, according to previous reports, the proliferation of hPSCs begins 2 days after passaging (42), hES3 and hiPS2 were cultured for 2 days before the examination. Neither small molecule significantly affected KiPS-67 expression (Figure 1E).

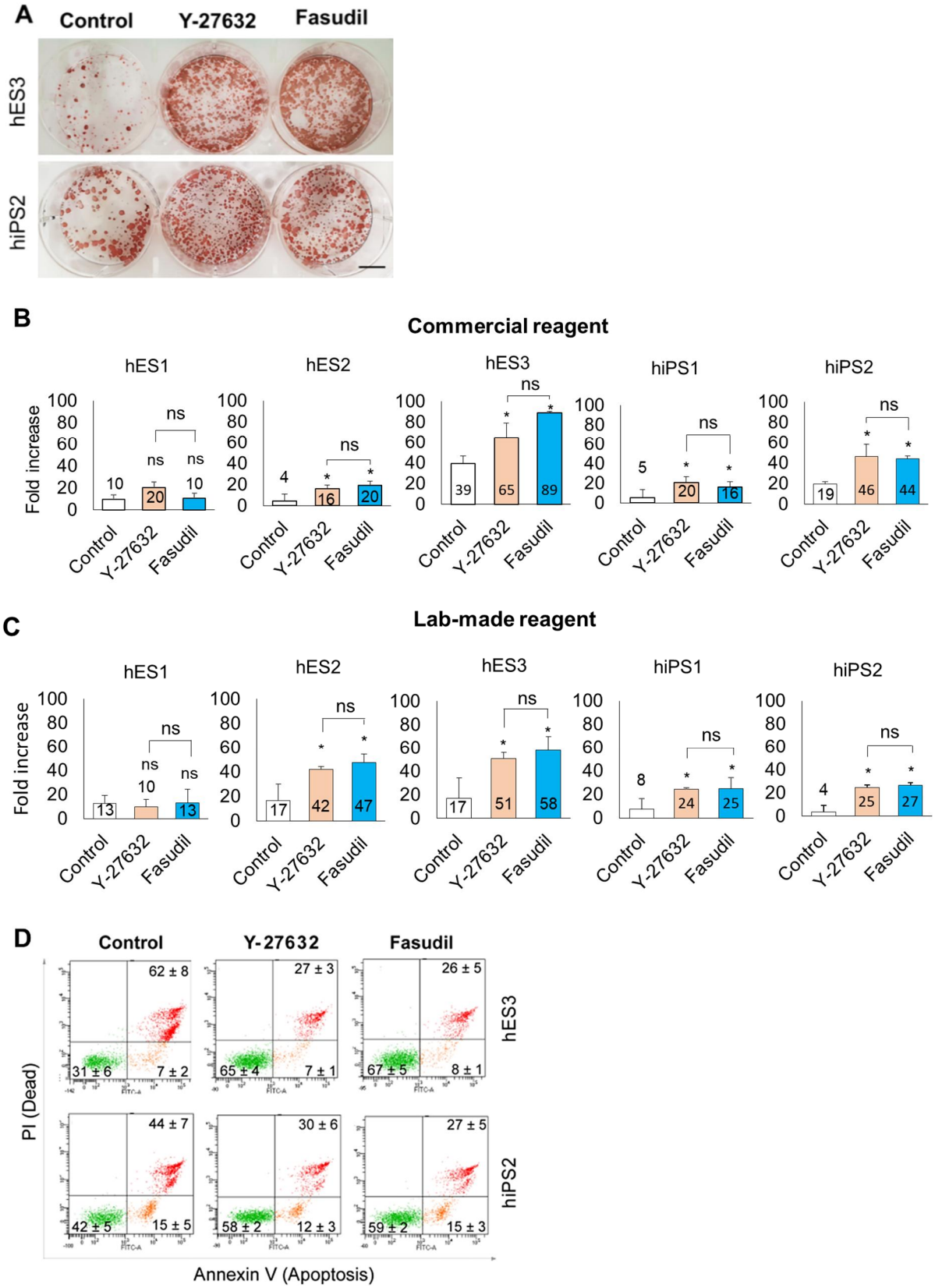
A
Control
Y-27632
Fasudil
hES3
hiPS2
B
Commercial reagent
hES1
hES2
hES3
hiPS1
hiPS2
Fold increase
ns
Control
Y-27632
Fasudil
C
Lab-made reagent
D
Control
Y-27632
Fasudil
62 ± 8
31 ± 6
7 ± 2
27 ± 3
65 ± 4
7 ± 1
26 ± 5
67 ± 5
8 ± 1
44 ± 7
42 ± 5
15 ± 5
30 ± 6
58 ± 2
12 ± 3
27 ± 5
59 ± 2
15 ± 3
PI (Dead)
Annexin V (Apoptosis)

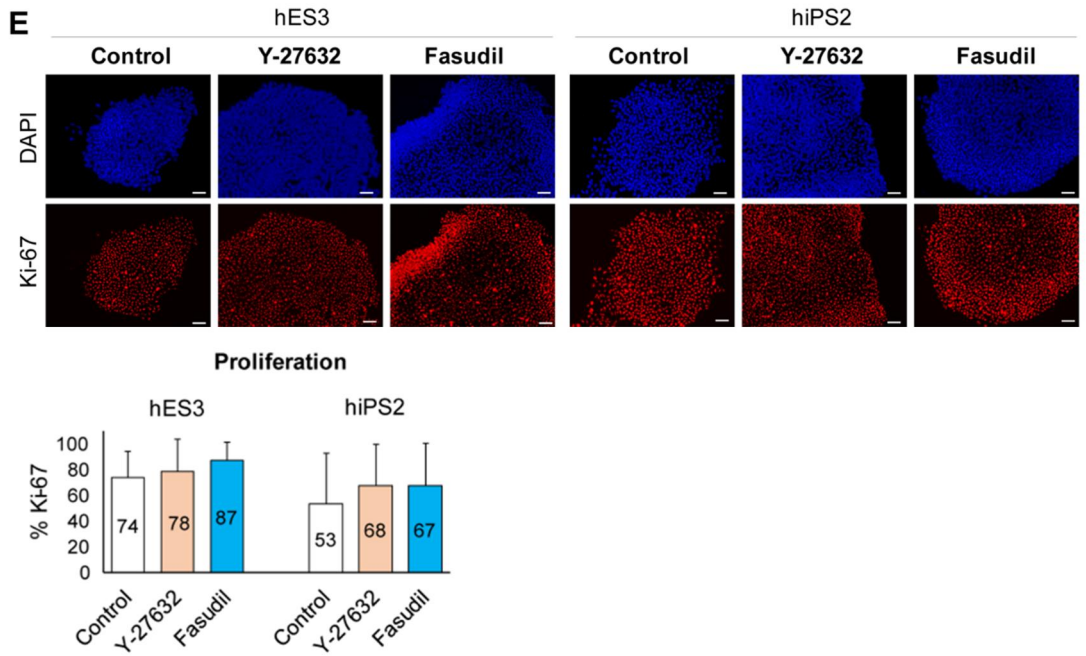

Figure 1. Fasudil enhances the cell growth of hPSCs. (A) ALP staining of hES3 and hiPS2 cells cultured with Y-27632 or fasudil. Treatment with fasudil or Y-27632 increased the size of PSC colonies. Scale bar = 10 mm. (B, C) Fold increase of initially seeded hESCs (hES1, 2, and 3) and hiPSCs (hiPS1 and 2) using commercial reagent (B) or lab-made reagent (C). Growth of all hPSC lines except hES1 increased in response to fasudil or Y-27632 (*: $p < 0.05$, 3 biological replicates). (D) Analysis of live and apoptotic hES3 and hiPS2 cells (%) 24 hours after seeding at 1×10^4 cells/cm^2. Compared with the control group, apoptotic cells decreased when treated with fasudil (*: $p < 0.05$; 3 biological replicates). (E) Cell proliferation was measured using immunofluorescence (upper) and flow cytometry (below) to examine Ki-67 expression in hES3 and hiPS2 cells 2 days after seeding. There were no significant differences between the groups (3 biological replicates). Scale bar = 100 μm.

2) Maintaining pluripotency following long-term fasudil treatment

To confirm that fasudil treatment does not affect pluripotency, five hPSC lines were sub-cultured with 10 uM of fasudil over 2 to 3 months and their pluripotency was examined. Representative PSC markers, including *OCT4, SOX2*, and *NANOG* were analyzed by qPCR. Individual PSC lines varied but gene expression levels did not differ significantly between the treatment groups (Figure 2A).

OCT4, SSEA4, and TRA 1–60 proteins were detected in all the cell lines by immunocytochemistry (ICC) (Figure 2B). Additionally, karyotyping revealed typical chromosome arrangements (Figure 2C). Finally, we injected the five cell lines into immunosuppressed mice (NSG, Jackson Laboratory, Bar Harbor ME) to examine teratoma formation. All the cell lines generated teratomas containing the three germ layers—ectoderm, mesoderm, and endoderm (Figure 2D). These findings demonstrate that fasudil does not affect the pluripotency of PSCs or cause chromosome aberrations and suggest that fasudil is a safe and effective small molecule ROCK inhibitor that can be used in long-term culture of PSCs.

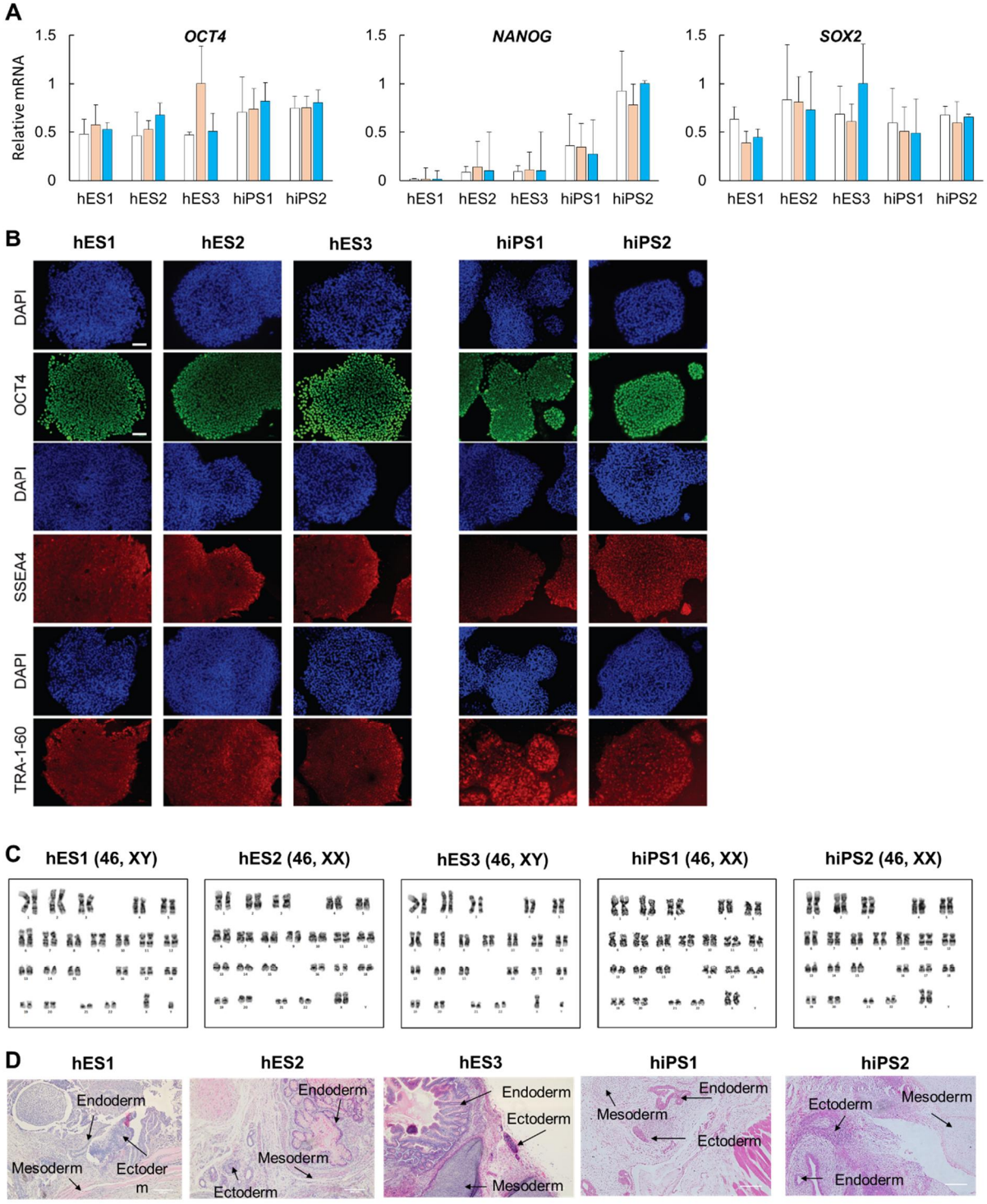

Figure 2. Characterization of hPSCs following fasudil treatment for 2 to 3 months. (A) Quantitative RT-PCR analysis of *OCT4*, *SOX2*, and *NANOG* expression relative to *GAPDH*. ROCK inhibitors were present only on the first day of passage. The difference between the two treatments was not significant (3 biological replicates, 3 technical replicates). (B) Immunofluorescence analysis examining OCT4,

SSEA-4, and TRA-1-60 expression, following fasudil treatment for 3 months. All 5 lines of PSC expressed the pluripotency markers. Nuclei were stained with DAPI (blue). Scale bars =100 μm. (C) G-banding karyotypes of hPSCs cultured with fasudil for 3 months. None of the five lines of PSC had any abnormality of karyotype. (D) Ectodermal, mesodermal, and endodermal tissue were associated with teratoma formation by five lines of hPSCs after 3 months in fasudil-treated culture. All three germ layers were formed. Scale bars = 200 μm.

3) The potential use of Fasudil in a variety of applications

To determine whether fasudil might be used in other PSC studies, we investigated the effect of fasudil on 3D aggregation and single-cell culture. To induce the aggregation of hPSCs for 3D culture, dissociated hES3 cells were cultured for six days in suspension (1.2×10^6 cells/ml, 1 ml/35 mm StemFit3D culture dish) using DMEM/F12 medium supplemented with KSR, to which fasudil or Y-27632 was added for the first 24 hours. After 24 hours, the hESCs (hES3) had begun to grow well as floating aggregates, but the control cells remained single (Figure 3A). With fasudil, aggregates formed in almost all the molds (98 ± 2%), and there was no significant difference in comparison with the cells in which Y-27632 was used (97 ± 4%). Also, there was no difference in the size of the aggregates, which were cultured for the aggregate sizes after a total of six days using Y-27632 (138.4 ± 18.6 μm) and fasudil (149.4 ± 10.2 μm).

To confirm the protective effect of fasudil on the growth of single hPSCs, hES3 cells were dissociated into single cells and seeded on a plate with Y27632 or fasudil. Cells were counted after seven days of culture. Treatment with either inhibitor substantially increased cell numbers (56 ± 13 and 49 ± 8 vs. 1 ± 0.6, $p < 0.05$) (Figure 3B).

In summary, fasudil appears suitable for use as a cheaper substitute for Y-27632 in stem cell studies.

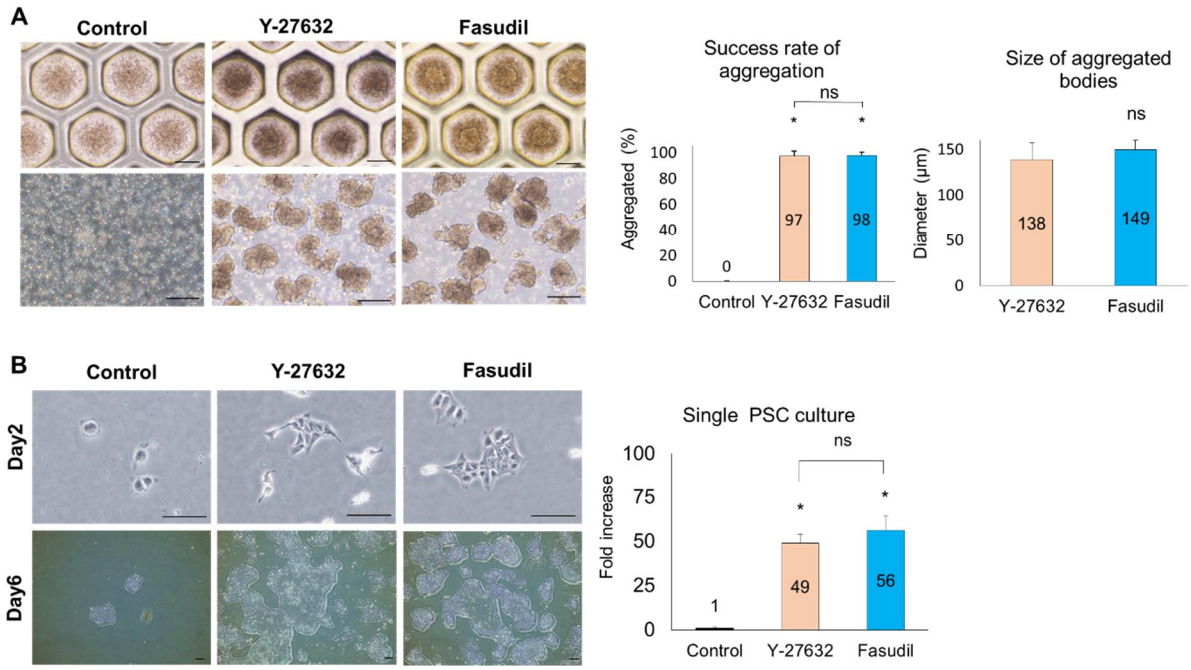

Figure 3. Other applications of fasudil. (A) Supportive effect of fasudil on hES3 survival and growth in suspension culture. The fasudil-treated groups and Y-27632-treated groups were similar in the rate of formation of cell aggregates and their size; the control cells did not form aggregates. Scale bar = 200 μm (*: $p < 0.05$, 2 biological replicates, 7 technical replicates). (B) Seven-day cultures of single hES3 cells on vitronectin-coated culture plates in the presence of 10 μM Y-27632 or fasudil. Scale Bar = 200 μm. The growth of hPSCs was faster with Y-27632 or fasudil than in the untreated control (*: $p < 0.05$, 3 technical replicates).

5. Discussion

ROCK proteins consist of two subunits, ROCK1 and ROCK2, and play crucial roles in numerous cellular functions, including cell contraction, actin organization, cell migration, and proliferation (43). Cell-cell interactions are essential for colony formation, and a study of the roles of the Rho-ROCK-Myosin signaling axis in cell-cell interactions has suggested that signaling mechanisms differ between multipotent and non-pluripotent cell lines (44, 45), and those ROCK inhibitors are useful for culturing human pluripotent stem cells (hPSCs); most researchers use Y-27632 as their preferred ROCK inhibitor.

The ROCK inhibitor fasudil was initially used in the treatment of cancer (46). Since then, Y-27632, which is more effective in cancer, was developed and used on hPSCs. We were interested in why Y-27632 is the normal choice for PSC studies despite the lower cost of fasudil and its known ability to improve hPSC survival. However, fasudil was not characterized by PSCs through long-term culture.

In an experiment involving ROCK inhibitors, we observed that fasudil promoted hPSC growth. This led to the examination of the action of fasudil on undifferentiated hPSC cultures. We found that when PSCs were frozen and thawed, simple supplementation with fasudil significantly improved survival due to inhibition of the ROCK pathway, which is reported to be one of the most important signaling pathways affecting hPSC survival (47). Fasudil also improved hPSC growth and the formation of 3D aggregates by preventing apoptosis of dissociated hPSC. The effect of fasudil seems to be due to inhibition of ROCK, which promotes depolymerization of actomyosin, and polymerization of actomyosin is essential for cell survival after detachment (48).

The PSC growth-promoting effects of the ROCK inhibitors varied depending on cell lines. Especially, hES1 did not increase cell growth compared with untreated control. Because the ROCK signal induces cell apoptosis through pMLC and p-cofilin pathway (37), the various expression levels of ROCK, pMLC, and p-cofilin could influence cell growth depending on cell lines (49-51).

We found that inhibition of ROCK by fasudil allowed for xeno-free long-term culture of hPSCs by maintaining correct gene expression, protein location, function, and karyotype.

[Chapter II was prepared based on PLoS ONE 15(5): e0233057, The Rho-associated kinase inhibitor fasudil can replace Y-27632 for use in human pluripotent stem cell research]

Chapter III-1.

Study of mitochondrial DNA mutations in induced pluripotent stem cells derived from diabetic patients

1. Abstract

Diabetes mellitus (DM) is a group of metabolic disorders characterized by hyperglycemia in which various genetic and environmental factors cause progressive loss of β-cell or function of insulin. Although many researchers are researching the treatment of diabetes using induced pluripotent stem cells (iPSCs), it is not known exactly how mitochondrial DNA (mtDNA) mutations tend to appear in iPSCs derived from diabetic patients. It has been reported that pathogenic mutations in mtDNA can cause DM, which means that mtDNA mutations can also adversely affect the use of iPSCs as cell therapy for diabetes (52).

In this part, we obtained fibroblasts, PBMCs, and pancreatic cells from each of three types 2 diabetic patients and three non-diabetic controls, and established iPSC clones therefrom. Then, mtDNA mutations in parental cells and iPSCs were analyzed by mtDNA sequencing using the Miseq platform. As a result, various mtDNA mutations were found in iPSC regardless of the presence or absence of disease, and most of these mutations did not exist in parental cells. Also, there was no diabetic or tissue-specific mtDNA mutation. Interestingly, when mtDNA mutations of non-diabetic and diabetic patients were compared, more homoplasmic mtDNA mutations were found in diabetic patients, and the average heteroplasmy was higher in diabetic patients.

2. Introduction

Diabetes mellitus (DM) is a metabolic disease characterized by high blood sugar levels over a prolonged period (53). Diabetes is classified into type 1 and type 2. Type 1 diabetes is a disease in which the β-cells in the pancreatic islets of Langerhans are destroyed and unable to produce insulin. Type 2 diabetes (T2D) accounts for most diabetic patients and is classified as a serious geriatric disease because it is difficult to treat (54). In T2D, insulin resistance causes skeletal muscle, liver, and adipose tissue to fail to respond to insulin, resulting in elevated blood sugar (55, 56). In addition, excessive insulin production and hyperglycemia due to T2D can damage β-cells, leading to progressive impairment of insulin secretion (57, 58). A variety of treatments have been developed for T2D, including drugs, surgical treatments, organ/tissue transplantation, and cell therapy. In the later stages of T2D, islet transplantation is the most effective treatment, but the lack of donors limits its large-scale clinical application. To overcome this problem, the use of induced pluripotent stem cells (iPSCs) from the patient's autologous cells can be considered (59, 60).

iPSCs can be generated from somatic cells such as fibroblasts, peripheral blood mononuclear cells (PBMCs), and other tissue cells by transducing transcription factor genes such, as *OCT4*, *SOX2*, *KLF4*, and *c-MYC* (61). The iPSCs have great potential for use in drug discovery, disease modeling, and cell therapy, because of their ability to proliferate indefinitely and differentiate into various cell types (62). Because of these characteristics, iPSCs have value as patient-specific cell therapy and can also be differentiated into pancreatic cells, which are useful for anti-diabetic drug development, diabetic disease modeling, and clinical treatment. However, abnormalities of the genome, such as aneuploidy, sub-chromosomal copy number variations, and single nucleotide variations in iPSCs limit their clinical use (63).

Mitochondria are key organelles responsible for adenosine triphosphate (ATP) production within cells and have an independent genome called mitochondrial DNA (mtDNA) (64). The mtDNA encodes many genes essential for oxidative phosphorylation and cellular energy production (65). The mutation frequency of mtDNA is 10 to 20 times higher than that of nuclear DNA, and mtDNA mutations cause various human inherited diseases (66). Because mtDNA is a multi-copy genome, it often represents a heteroplasmic genotype in which both the healthy and the mutated allele are present in the same cell. Each tissue has a different threshold level for mtDNA mutations, and the pathology may differ depending on the heteroplasmy of the mtDNA mutations (65). Because mtDNA mutations can

directly affect mitochondrial function, they result in a variety of diseases, such as Mitochondrial Encephalopathy lactic acidosis, stroke-like episodes (MELAS), Leber Hereditary Optic Neuropathy (LHON), and Pearson Syndrome (PS) (67). It has been reported that DM can also be caused by several pathogenic mtDNA mutations (68). Although mtDNA mutations present in diabetic-derived iPSCs may also have negative implications for future cell therapy, disease modeling, and drug screening studies, how mtDNA mutations in diabetic-derived iPSCs manifest have not been reported yet.

Thus, in the part III-1 studies, we generated iPSC lines from fibroblasts, PBMCs, and pancreatic cells of T2D patients and analyzed the mtDNA for mutations. In addition, we induced iPSC from non-diabetic patients and compared them with mtDNA mutations in diabetic patients.

3. Materials and Methods

1) Ethics and Governance

For experiments involving human samples, informed consent was obtained from participants and approved by the institutional review board (IRB: 2017-0260 and 2019-0117) of the Asan Medical Center. The patient information is presented in Table 1.

2) Generation of iPSCs

Somatic cells were induced into iPSCs with a CytoTune-iPS Reprogramming Kit (Life Technologies, Grand Island, NY) according to the manufacturer's protocol. iPSC colonies were selected and expanded with stemMACS medium (Miltenyi Biotec, Bergisch Gladbach, Germany).

3) mtDNA sequencing by MiSeq

The mtDNA was amplified using two primer sets as previously described (69, 70): mt3163F-GCCTTCCCCCGTAAATGATA and mt11599R-TGTTTGTCGTAGGCAGATGG; mt11506F-TCTCAACCCCCTGACAAAAC and mt3259R-TATGCGATTACCGGGCTCT. PCR conditions using Platinum™ SuperFi™ PCR Master Mix (Invitrogen, Carlsbad, CA) included an initial denaturation at 95°C for 5 minutes, 35 cycles of denaturation at 95°C for 20 seconds, annealing at 56°C for 20 seconds, extension at 68°C for 4 minutes, and a final extension at 68°C for 3 minutes. The concentration of the PCR products was measured using a Qubit 2.0 Fluorometer (Invitrogen). The DNA was used for library preparation using the Nextera XT DNA Kit (Illumina, San Diego, CA). Sequencing was performed on the Illumina MiSeq platform and the data were analyzed using NextGENe software. mtDNA sequencing was done as previously described (19).

4) Statistical analysis

Statistical comparisons between the two groups were made using Student's two-tailed t-test or two-tailed paired t-test. One-way ANOVA with Tukey post hoc analysis using Prism™ 5 software (GraphPad, San Diego, CA) was applied when more than two groups were compared. Data are expressed as the mean ± standard deviation (SD).

Table 1. Information of patients

Disease	Lab ID	Age	Sex	Clinical information
T2D	T2D-1	62-yrs	Male	NA
	T2D-2	71-yrs	Female	NA
	T2D-3	73-yrs	Female	NA
ND	ND-1	49-yrs	Female	benign/mild cancer
	ND-2	56-yrs	Female	NA
	ND-3	25-yrs	Male	NA

*NA: not applicable

4. Results and Conclusions

1) mtDNA mutations in iPSC clones derived from T2D patients

First, to investigate the presence of specific mtDNA mutations in T2D disease, we isolated fibroblasts (Fib), PBMCs (Blo), and pancreatic cells (Pan) from three T2D patients (T2D-1, 2, and 3), generated 34 iPSC clones, and detected 30 mtDNA mutations. We quantitatively evaluated the mutations in each clone and compared them with the parental cells. We were unable to obtain pancreatic cells from the T2D-1 patient because the condition of the pancreas was not suitable (Table 2).

Table 2. mtDNA mutations in iPSCs derived from patients with T2D

Subject	Cell origin	Position	Locus	Effect	Major haplotype	Parental cells (%)	Individual iPSC clone (%)				
							1	2	3	4	5
T2D-1 (M8a2c) 62-yrs Male	Fib	3315	ND1	syn	G	ND			A(48)		
		5226	ND2	non-syn	G				A(100)	ND	ND
		9018	ATPase6	syn	T		C(39)				
		12650	ND5	non-syn	T			C(56)			
	Blo	2613	16S	rRNA	T	ND	C(100)				C(100)
		10400	ND3	syn	T						C(100)
		11002	ND4	syn	A		G(100)				C(100)
		16005	ATT/P	mitoTIP 25.60%	T				ND	ND	C(7)
		16129	ATT/CR	non-coding	G			A(78)			
T2D-2 (B5a2a2) 71-yrs Female	Fib	5654	A	mitoTIP 29.80%	T	C(3)	C(13)	C(10)			
		5655	A	MitoTIP 26.70%	T						
		6207	COI	non-syn	T	C(6)				ND	
		9928	COIII	non-syn	A		G(11)				
		11976	ND4	non-syn	A		G(64)	G(55)			
		13726	ND5	non-syn	G						T(13)
		14260	ND6	syn	A		G(100)	G(100)	G(100)		
	Blo	874	12S	rRNA	G	ND		A(5)			
		2220	16S	rRNA	A				G(8)		
		4703	ND2	syn	T						C(5)
		6458	COI	syn	C						T (100)
		6678	COI	non-syn	A		G(100)				
		7970	COII	non-syn	G		A(13)				
		13312	ND5	non-syn	T					C(75)	
		14900	Cytb	non-syn	G					A(13)	
	Pan					ND	ND	ND	ND	ND	ND
T2D-3 (B4b1a1c) 73-yrs Female	Blo	6023	COI	syn	A	G(2)	ND	ND	ND	ND	
		10535	ND4L	syn	T	C(50)					
	Pan	302	CR:HVS2/	non-coding	A		ND	ND	ND	C(31)	
		9591	COIII	Non-syn	G						A(55)
		10535	ND4L	syn	T	C(55)					

*ND: not detected; Grey block: no iPSC clone, %: heteroplasmy

Two origins were obtained from the fibroblast and blood cells, and in total, 10 clones, including 5 fib-iPSC and 5 blo-iPSC clones, were obtained from the iPSCs of the T2D-1 patient. Three origins from fibroblast, blood, and pancreatic cells, and 5 iPSC clones each from fibroblast, blood, and pancreatic cells, a total of 15, were obtained from T2D-2 patients. Also, from the T2D-3 patient, two origins from fibroblast and pancreatic cells, and 4 blo-iPSC and 5 pan-iPSC clones were obtained. There were no mtDNA mutations shared between original cells and iPSCs (Figure 4A). We also analyzed whether there were mtDNA mutations shared among the iPSC clones to determine the presence of T2D disease-specific mtDNA mutations. Several mutations were shared among the iPSC clones within tissues from each individual (Table 2 grey color), whereas no mutations were shared among iPSCs of different origins (Figure 4B). Next, we investigated whether there were mutations shared among T2D patients (Figure 4C). There were no mutations shared among iPSCs derived from different patients.

Finally, we compared mtDNA mutations in iPSCs depending on the origin cells to determine whether tissue-specific mutations occur frequently in T2D diseases (Figure 4D). In fibroblast-derived iPSCs, an average of 0.8 mtDNA mutations per line in T2D-1 patients and 1.8 mtDNA mutations were found in T2D-2 patients. In blood-derived iPSCs, an average of 1.4 mtDNA mutations was found in T2D-1 patients and 1.6 were found in T2D-2 patients. No mutations were found in T2D-3 patients. Interestingly, fewer mtDNA mutations were found in iPSCs derived from pancreatic cells compared with the other origins (T2D-2 = 0, T2D-3 = 0.3).

To determine whether the mtDNA mutations found in pancreatic cell-derived iPSCs are actually fewer, we further established iPSCs from pancreatic cells of four additional patients (Pan1-4) and investigated mtDNA mutations (Figure 4E). The average number of mutations in pancreatic cell-derived iPSC clones was 1.77, which was not significantly different from fibroblast-iPSCs (1.3) or PBMC-iPSCs (1.5). Since there was no significant difference in the number of mtDNA mutations in iPSCs for each derived tissue, we decided to use PBMC-derived iPSCs that are relatively easy to obtain from patients in future differentiation studies.

Our results suggest that mtDNA mutations in iPSCs occur randomly irrespective of original cells and that mutations could not be predicted throughout the parental cells.

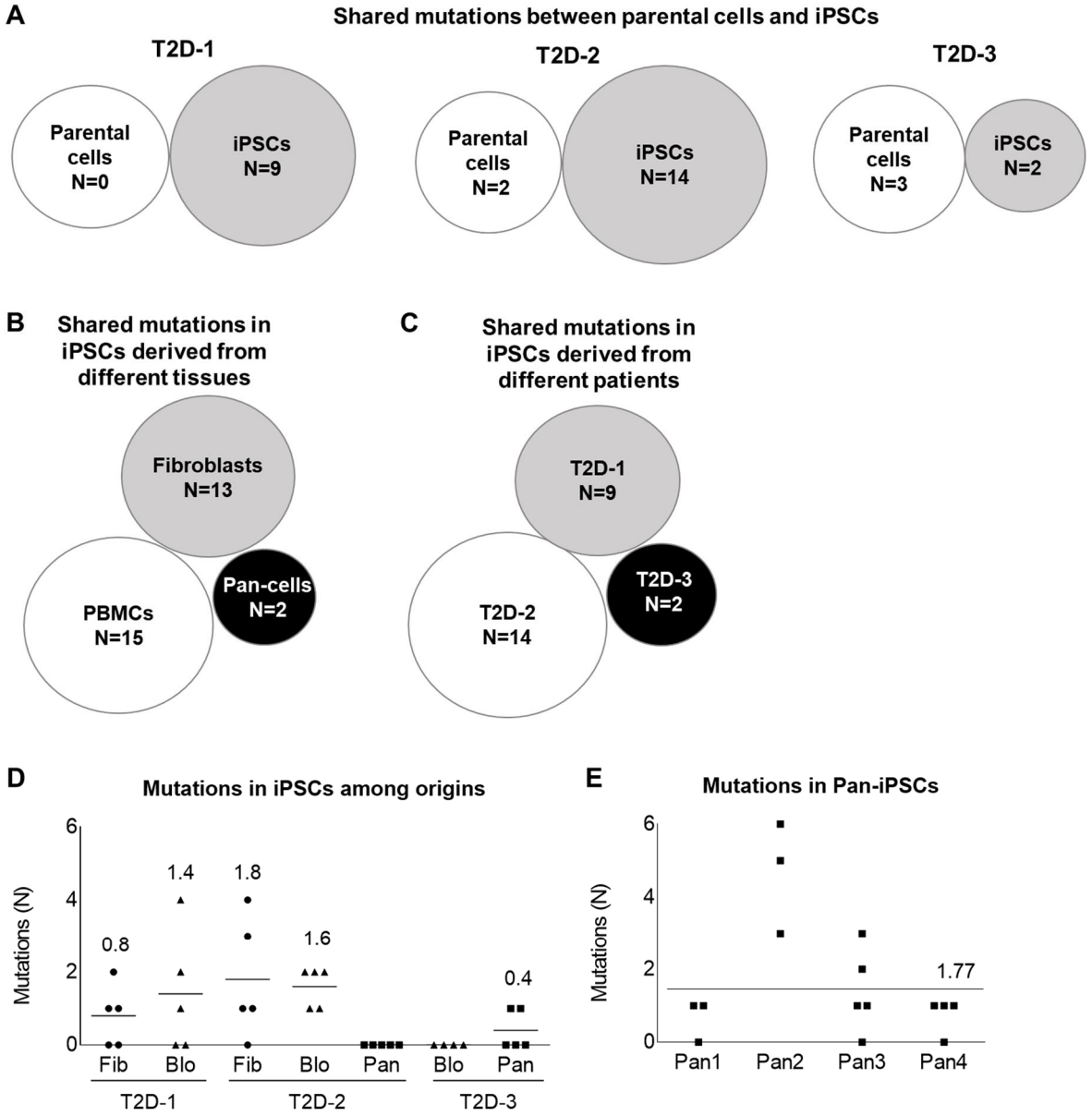

Figure 4. mtDNA mutations in T2D patients. (A) Venn diagram showing the absence of shared mtDNA mutations between origin cells and iPSCs. N=the number of mutations. (B) Venn diagram showing no mtDNA mutations shared between iPSCs of origin cells. (C) Venn diagram showing no shared mtDNA mutations among iPSC clones from individual patients. (D) The number of mtDNA mutations in iPSCs depends on different original cells. (E) The number of mtDNA mutations in iPSCs derived from a pancreatic origin. The average number of mtDNA mutations in the whole pan-iPSC clones was 1.77, which was not significantly different from that of iPSCs derived from other tissues.

2) mtDNA mutations in iPSCs derived from patients with non-diabetes

Next, we isolated Fib, Blo, and Pan from 3 ND patients and established iPSC clones. Although ND patients do not have diabetes, they have undergone biopsy due to other diseases, and accurate clinical information could not be obtained. Three to five clones were established in each line. Nine parental cell lines and 30 iPSC clones were analyzed for mtDNA mutations (Table 3).

Three mutations were identified in Fib of ND-1; mt1351, mt10158, and mt15077. Even 45% heteroplasmy in Fib, iPSC clones had not carried the same mutation indicating any shared mutation with parental cells. Mutation in mt15077 was shared with Blo of the same individual with similar heteroplasmy (14% and 12%), but any iPSC clones were not carried this shared mutation. However, mt14287C>T mutation was shared among iPSC clones from Fib, Blo, and Pan with high frequency, which 12 clones out of 13 clones were carried it with 14% ~ 50% heteroplasmy.

There was no shared mutation among parental cells in ND-2. Mt2976G>A with 48% heteroplasmy was identified in Pan, but any iPSC clones had detected the mutation. No mutation was identified in three different parental cells in ND-3. Seven iPSC clones out of 12 were carried mtDNA mutations. Mt4298G>A encoded tRNA was shared with two iPSC clones from Pan, which was 83.5% pathogenicity in Mito TIP (https://www.mitomap.org/MITOMAP).

Table 3. mtDNA mutations in iPSCs derived from patients with ND

Subject	Cell origin	Position	Locus	Effect	Major haplotype	Parental cells	Individual iPSC clones (%)				
							1	2	3	4	5
ND-1 (D4b2a2a) 49-yrs Female	Fib	1351	12S	rRNA	G	A (45)	T (36)	T (44)	T (45)	T (47)	T (39)
		10158	ND3	non-syn	T	C (6)					
		14287	ND6	syn	C						
		15077	Cytb	non-syn	G	C (14)					
	Blo	7780	COII	syn	A		G (78)				
		13726	ND5	non-syn	G			T (7)			T (4)
		14287	ND6	syn	C			T (35)	T (44)	T (14)	T (44)
		15077	Cytb	non-syn	G	A (12)					
		15773	Cytb	non-syn	G					A (24)	
	Pan	9478	COIII	non-syn	T				C (100)		
		13726	ND5	non-syn	G		T (12)				
		14268	ND6	syn	G	ND	T (14)	T (100)	T (100)		
		14287	ND6	syn	C		T (34)	T (50)	T (45)		
		15087	Cytb	non-syn	A			G (4)			
		15096	Cytb	non-syn	T			C (4)			
ND-2 (M7a1a7) 56-yrs Female	Fib	13726	A	mitoTIP 29.80%	G	T (7)					
	Blo					ND					
	Pan	2976	16S	rRNA	G	A (48)					
		4028	ND1	non-syn	T		G (5)	G (12)			G (5)
		6026	COI	syn	G		C (5)			ND	
		11379	ND4	non-syn	T						C (6)
		14343	ND6	non-syn	C		A (16)		A (23)		
ND-3 (D4f1) 25-yrs Male	Fib	3047	16S	rRNA	G	ND	A (8)				
	Blo	13107	ND5	non-syn	C		A (40)	A (8)		A (39)	
	Pan	4298	I	mitoTIP pathogenic (83.50%)	G	ND	A (52)	ND		A (47)	
		4713	ND2	ND2:G82TERM	G				A (74)		

*ND: not detected; Grey block: no iPSC clone, %: heteroplasmy

3) Comparison of mtDNA mutations in iPSCs between type 2 diabetic and non-diabetic

We compared mtDNA mutations in iPSC clones between patients with ND and T2D to determine the difference in the mtDNA mutation pattern. The number of mtDNA mutations per iPSC clone was not different in ND (1.2) and T2D (0.9) (Figure 5A). 61% of T2D-iPSC clones (21/34) carried one or more mtDNA mutations, whereas 80% (24/30) in ND-iPSCs (Figure 5B). Next, we analyzed the heteroplasmy of the mtDNA mutations found in iPSCs to compare the pathogenicity of mtDNA mutations. Since the threshold differs according to the position of the mtDNA mutation, we decided to use 50% heteroplasmy, which may be universally pathological as a standard. So, we compared by dividing it into less than 50% heteroplasmy group, which is less likely to be dangerous, and more than 50% heteroplasmy group, and homoplasmy group (13, 71). Only 43% of mtDNA mutations identified in T2D-iPSCs (13/30) contained less than 50% heteroplasmy and 37% (11/30) with homoplasmy (Figure 5C). Interestingly, mtDNA mutations with homoplasmy in ND accounted for only 8% (3/37). We also analyzed the proportion of heteroplasmy of mtDNA mutations in iPSCs from individual T2D patients to compare differences between T2D patients (Figure 5D). The proportion of heteroplasmy was different among the three T2D patients, but the proportion of mtDNA mutations with more than 50% heteroplasmy was higher than that of ND. The heretoplasmy average in each ND patients differed significantly only in ND-1 and ND-2 (Figure 5E). The averages of mtDNA mutations of each T2D patient were 75.3, 43.5, and 43%, respectively, and there was no significant difference between them (Figure 5F). Comparing the average heteroplasmy of iPSC clones with mutations in ND and T2D, it was significantly higher in T2D (52%) compared to ND (34%) ($p < 0.05$, Figure 5G). Additionally, the probability of obtaining an iPSC clone with homoplasmic mtDNA mutation in T2D was 24% compared to only 7% in ND (Figure 5H).

The distribution of mtDNA mutations showed that non-synonymous (non-syn) mutations resulting in changes in amino acid coding were 46% (17/37) in ND and 37% (11/30) in T2D (Figure 5I). The synonymous (syn) mutations were 46% (17/37) in ND and 33% (10/30) in T2D. For mutations in the RNA region, it was only 8% (3/37) in ND compared to 23% (7/30) in T2D. Mutations in the D-loop, a non-coding region, were found only in T2D (7%, 2/30).

Despite the limitation of only three diabetic patients, these results suggest that homoplasmic mtDNA mutations are found more frequently in iPSC clones from T2D patients than in ND patients although mtDNA mutations in iPSCs occur randomly regardless of parental cells.

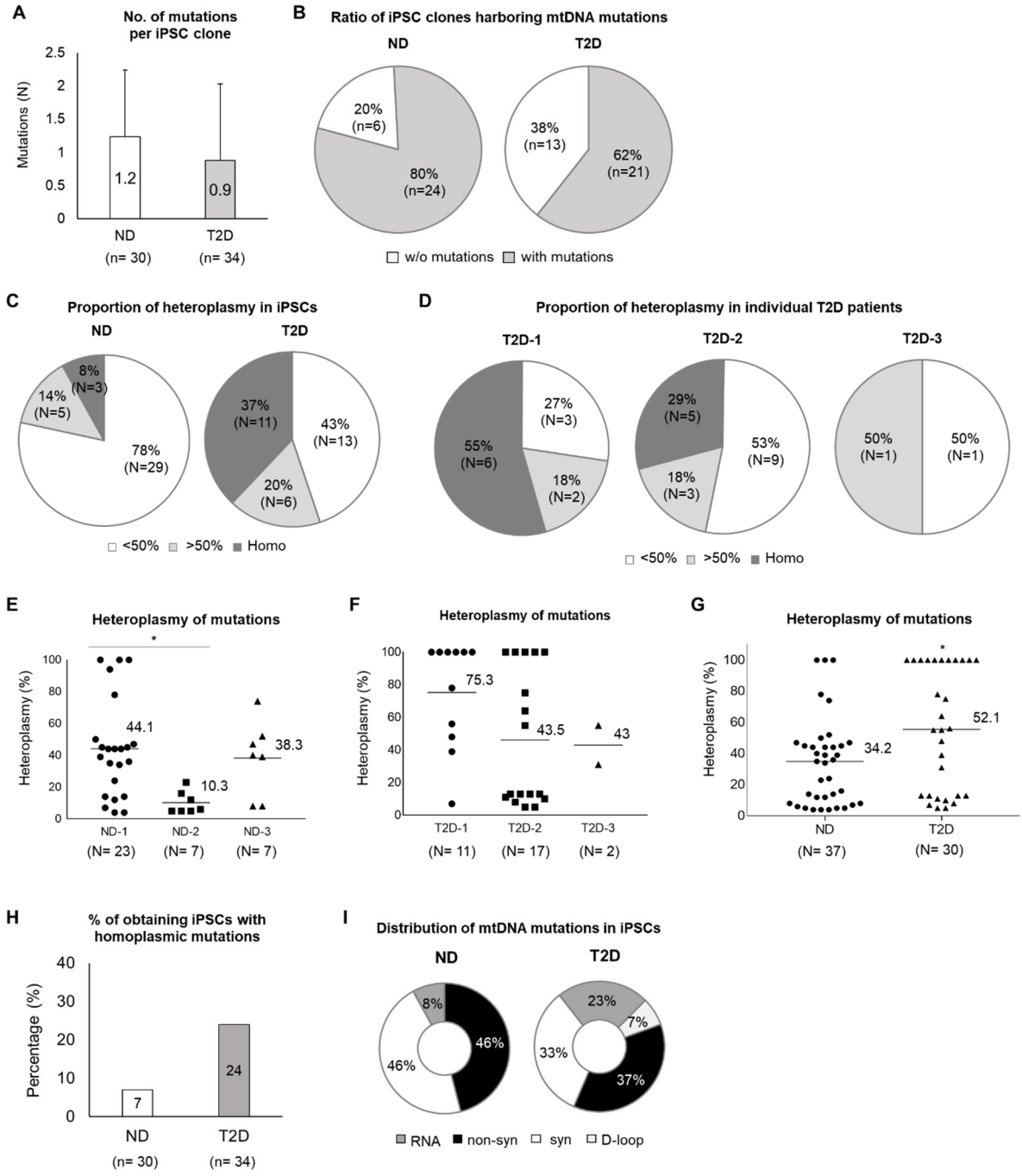

Figure 5. mtDNA mutations in patients with ND- and T2D-iPSCs (A) The average number of mtDNA mutations in iPSC clones derived from patients with ND and T2D. (B) The proportion of iPSCs with and without mtDNA mutations in ND and T2D patients. n=the number of iPSC clones. (C) Heteroplasmy proportion of whole mtDNA mutations in iPSCs. N=the number of mtDNA mutations (D) Heteroplasmy proportion of mtDNA mutations in iPSC clones derived from individual T2D patients. (E) Heteroplasmy distribution of mtDNA mutations in individual ND patients. The average of

heteroplasmy of ND-1 was significantly higher than that of ND-2 (*: $p < 0.05$). (F) Heteroplasmy distribution of mtDNA mutations found in each T2D patient. There were no significant differences between diabetic patients. (G) Heteroplasmy distribution of mtDNA mutations found in ND- and T2D-iPSCs. The heteroplasmy of mutations found in T2D was higher than that of ND (*: $p < 0.05$). (H) Probability of obtaining iPSCs with homoplasmic mtDNA mutations. (I) Distribution of mtDNA mutations in ND and T2D. The ratio of mutations in the RNA region was higher in T2D than in ND (23% vs. 8%).

Chapter III-2.

Study of *in vitro* pancreatic differentiation related to mitochondrial DNA mutations

1. Abstract

Although many studies have been conducted to cure diabetes using induced pluripotent stem cells, it has not been investigated whether mitochondrial genome (mtDNA) abnormalities in iPSCs affect pancreatic β-cell differentiation and function. mtDNA resides within the mitochondria, which act as the power plant of our cells, and encodes several energy production-related proteins. Mutations in mtDNA can affect these mitochondrial functions, which can impair survival, differentiation, and function.

In this part, we selected iPSC clones from one type 2 diabetic patient and analyzed the morphology of iPSC and mtDNA copy numbers according to mtDNA mutation. All iPSC clones with or without mutation showed normal PSC morphology, but the higher the mtDNA mutation heteroplasmy, the lower the mtDNA copy number. Then, we differentiated them into pancreatic lineages, and as a result, confirmed that mtDNA mutation inhibited differentiation and impaired mitochondrial respiratory function. In addition, it was confirmed that metabolites such as glucose-6-phosphate, malate, and NAD were decreased in pancreatic β-cells differentiated from mutant iPSCs. Finally, we investigated the function of pancreatic β-cell including insulin production and glucose-stimulated insulin secretion and confirmed that mtDNA mutation can impair pancreatic dysfunction.

2. Introduction

Although mtDNA is small at only 16,569 base pairs, it contains 37 genes that encode 13 proteins, 22 tRNAs, and 2 rRNAs. All mtDNA gene-encoded proteins make up the subunits of the enzyme complexes of the oxidative phosphorylation system, allowing the mitochondria to act as the powerhouse of cells (72). Moreover, mtDNA has a higher mutation rate than those observed in genomic DNA (66). It has been reported that individual iPSC clones, each derived from a single cell, can carry mtDNA mutations that cause functional abnormalities, which are not generated during reprogramming but are already present in individual parental cells (15). Also, these somatic mutations tend to increase with age, which is associated with accumulated damage or replication errors in mtDNA (16).

More than 20 mtDNA mutations associated with DM have been reported, including mt3243 mutation in which A is replaced by G at the position encoding leucyl-tRNA^{UUR23} (16). In addition, mitochondrial dysfunction may have a direct effect on DM, because ATP, cAMP, NADPH, and other metabolites produced in mitochondrial metabolism act as additive signals regulating insulin secretion in β-cells (73). Therefore, the presence of mtDNA mutations in iPSCs can be problematic when using iPSC as autologous cell therapy or disease modeling of DM (74, 75).

Because iPSCs can be induced in patient cells and have pluripotency, they can be differentiated into various cell types and can proliferate indefinitely, so their potential as a cell therapy is in the spotlight. iPSCs can also be derived from diabetic patients, and in the previous chapter, it was confirmed that iPSCs derived from diabetic patients had more mtDNA mutations with higher heteroplasmy and more homoplasmic mtDNA mutations compared to non-diabetic patients. Although studies to treat diabetes by differentiating iPSCs derived from diabetic patients into pancreatic β-cells have been actively conducted until recently, it has not yet been known how the somatic mtDNA mutation with high heteroplasmy found in diabetic patient-derived iPSCs affects pancreatic differentiation and function (4). It can be a hurdle to the use of iPSCs as patient-specific cell therapy. Therefore, we tried to investigate how mtDNA mutation with high heteroplasmy affects the differentiation of iPSCs into pancreatic cells and the function of differentiated pancreatic cells.

In the part III-2 study, we selected iPSCs derived from one type 2 diabetic patient and evaluated its morphology, mtDNA mutational status, and copy number variation. Furthermore, iPSCs were induced to differentiate into pancreatic progenitor cells (PPCs) and the expression of differentiation markers and mitochondrial activity were measured. Finally, the production of insulin, energy-related

metabolites, and glucose-stimulated insulin secretion (GSIS) were analyzed to confirm the association between mtDNA mutation and the function of differentiated pancreatic β-cell. A functional analysis was done after the iPSC-derived PPCs were differentiated into pancreatic β-cells.

3. Materials and Methods

1) Quantification of mitochondrial copy number

mtDNA copy number was determined using the Absolute Human Mitochondrial DNA Copy Number Quantification qPCR Assay Kit (ScienCell, Carlsbad, CA) according to the manufacturer's instructions. mtDNA copy number was calculated as the ratio of the number of mitochondrial DNA copies to that of nuclear DNA.

2) Pancreatic progenitor cell differentiation

Pancreatic progenitor cells were derived by in vitro differentiation of iPSCs as previously described (76). Briefly, hPSCs were seeded at 40% to 50% confluency onto 6-well plates coated with vitronectin in a StemMACS medium. Three days after plating, for definitive endoderm differentiation, the medium was changed to step 1 medium; RPMI1640 (Life Technologies) supplemented with 2% fetal bovine serum (FBS, Life Technologies), 100 ng/ml activin A (Peprotech, Cranbury, NJ) and 3 μM CHIR99021 (Peprotech) and incubated for one day. For the following 2 days, the cells were cultured with step 2 medium: RPMI1640 supplemented with 10% FBS and 100 ng/ml activin A. For pancreatic progenitor cell differentiation, the medium was changed to step 3 medium: IMEM (Life Technologies) supplemented with 1% B27, 50 ng/ml noggin (Peprotech), 1 μM dorsomorphin (Sigma-Aldrich), 2 μM retinoic acid (Sigma-Aldrich), and 10 μM SB431542 (Selleckchem, Houston, TX) for 7 days. The differentiation process also included a 10 μM fasudil treatment. The medium was replaced every day.

3) Quantitative polymerase chain reaction (qPCR)

Total RNAs were isolated using RNeasy Mini Kits (Qiagen, Valencia, CA, USA), and reverse transcription was performed using cDNA synthesis kits (PCR Biosystems, London, UK). The results were confirmed by conventional real-time polymerase chain reaction (PCR) analysis. Quantitative reverse transcriptase PCR (RT-qPCR) was done using gene-specific primers, Power SYBR Green PCR Master Mix, and a QuantStudio 6 Flex Real-Time PCR System (Applied Biosystems, Foster City, CA, USA). The qPCR reactions were prepared in a final volume of 10 μl containing 5 μl SYBR Green master mix, 2 μl cDNA (50 ng/μl), 0.5 μl each forward and reverse primer (10 pmol), and 2 μl nuclease-free water. The annealing temperature was 56~60°C. The PCR data were analyzed and normalized relative to GAPDH expression using QuantStudio 6 and 7 Flex software (Applied Biosystems).

4) Flow cytometry

Cells were collected using 0.25% trypsin-EDTA and fixed with 10% neutral buffered formalin (BBC Biochemical, Mount Vernon, WA) for 30 min at room temperature. Fixed cells were washed twice with phosphate buffered saline (PBS, Hyclone, Chicago, IL, USA) and permeabilized with 0.05% Triton X-100 in 0.01 M sodium citrate for 30 min at room temperature. PDX1 primary antibody (Abcam, Cambridge, UK) was diluted at 1:200 in PBS containing 2% FBS and refrigerated overnight. Thereafter, the cells were washed three times with PBS and incubated for 1 h in the refrigerator with mouse anti-goat IgG H&L (1:500, Alexa Fluor 488, Abcam) and counted using a FACS (Canto II, BD Biosciences) (11). The FACS data were analyzed with FlowJo xV.0.7 software (Tree Star, Ashland, OR).

5) Assessment of mitochondrial respiratory function

Mitochondrial respiratory function was measured using an XF Cell MitoStress Test Kit and an XF24 Extracellular Flux Analyzer (Seahorse Biosciences, North Billerica, MA), as described previously (19). Mitochondrial OCR was measured by serial treatment with 1.5 μM oligomycin for ATP production (oligomycin OCR – basal OCR), 1 μM carbonyl cyanide 4-(trifluoromethoxy) phenylhydrazone (FCCP) for maximal respiration and reserve capacity (maximal OCR– basal OCR), and 0.5 μM antimycin A and 0.5 μM rotenone for non-mitochondrial oxygen utilization. Oxygen consumption was normalized to baseline oxygen consumption by measuring cell DNA.

6) Pancreatic β-cell differentiation

For pancreatic β-cell differentiation, dissociated PPCs (prepared as above; 1 × 106 cells/ml) were seeded into a StemFIT 3D culture dish (MicroFIT, Republic of Korea). Two days later, aggregates were transferred to a low attachment dish with an IMEM medium supplemented with 1% B27 (Gibco), 10 μM forskolin (Selleckchem), 10 μM dexamethasone (Sigma-Aldrich), 5 μM Repsox (Selleckchem), and 10 mM nicotinamide (Sigma-Aldrich) for 11 days. The differentiation process also included 10 μM fasudil treatment and the medium was replaced once every 3 days.

7) Immunocytochemistry

After pancreatic β-cell differentiation, spheroids were fixed in 10% neutral buffered formalin overnight in a refrigerator (2-8°C) and washed twice with PBS. Fixed aggregates were permeabilized and blocked with 0.05% Triton X-100 and 1% BSA in PBS for 30 minutes at room temperature. Insulin antibodies (Cell signaling technology, Danvers, MA) were diluted 1:100 in PBS containing 0.1% tween 20, and aggregates were incubated overnight in the refrigerator. After incubation with primary antibodies, aggregates were washed three times with PBS and incubated for 1 hour at room temperature with

secondary antibodies (Goat Anti-Mouse IgG H&L, 1:1000, Alexa Fluor 488, Abcam). Samples were imaged and captured using a ZEISS LSM 780 Laser Scanning Microscope (Zeiss, Oberkochen, Germany; Confocal Imaging Core Laboratory, ASAN Institute for Life Sciences, Seoul, Republic of Korea).

8) Validation of mtDNA mutations by Sanger sequencing

Validation of mtDNA mutation sites over 15% heteroplasmy was conducted independently by Sanger sequencing. The mtDNA regions containing mutations as determined by Miseq were amplified by PCR with the previously reported primer sets (77) using the 2X PCRBIO Ultra Kit (PCR Biosystems). The PCR products were purified by ExoSAP-IT™ PCR. Product Cleanup Reagent (Life Technologies) according to the manufacturer's instructions. Sanger sequencing of the PCR products was done by the Macrogen Corporation (Seoul, Republic of Korea). The data were analyzed using Sequencher v. 4.1 (Gene Codes Corporation, Ann Arbor, MI) (19).

9) Measurement of metabolites related to energy metabolism

The experiment was performed as previously described (78). Briefly, standard metabolites and internal standards were purchased from Sigma-Aldrich. All solvents including water were purchased from J. T. Baker. Cells were harvested using 1.4 mL of cold methanol/H_2O (80/20, v/v) after rapid, sequential washes with PBS and H_2O. The cells were then lysed by vigorous vortexing and 100 μL of 5 μM of internal standard ($^{13}C_5$-Gln) were added. Metabolites were extracted from the aqueous phase by liquid-liquid extraction after chloroform addition. The aqueous phase was dried using a vacuum centrifuge and the sample was reconstituted with 50 μL of 50% methanol before LC-MS/MS analysis. Metabolites related to energy metabolism were analyzed by LC-MS/MS equipped with a 1290HPLC (Agilent, Waldbronn, Germany), QTRAP 5500 (AB Sciex, Toronto, Canada), and a reverse-phase column (Synergi fusion RP 50 × 2 mm). Mobile phases A and B were 5 mM ammonium acetate in H_2O and 5 mM ammonium acetate in methanol, respectively. The solvent gradient was as follows: hold at 0% B for 5 min, 0% to 90% B for 2 min, hold at 90% for 8 min, 90% to 0% B for 1 min, then hold at 0% B for 9 min. LC flow was 70 μL/min except, for 140 μL/min between 7-15 min, and the column temperature was kept at 23°C. Multiple reaction monitoring (MRM) was used in negative ion mode and the extracted ion chromatogram (EIC) corresponded to the specific transition for each metabolite used for quantitation. The area under the curve of each EIC was normalized to that of the EIC of the internal standard. The peak area ratio of each metabolite to the internal standard was normalized by protein amount.

10) Analysis of insulin synthesis in pancreatic cells

Pancreatic β-cells were harvested and lysed in RIPA lysis buffer (EPIS BIO, Republic of Korea) containing phosphatase and protease inhibitors (Sigma-Aldrich). The cell lysates were then analyzed for insulin content using an insulin ELISA kit (ALPCO, Salem, NH), according to the manufacturer's protocol.

11) Glucose-stimulated insulin secretion (GSIS)

To perform GSIS, hiPSC derived pancreatic β-cells were preincubated with 0.5 mg/ml glucose in Krebs-Ringer HEPES buffer (130 mmol/L NaCl, 1.25 mmol/L KH_2PO_4, 1.25 mmol/L $MgSO_4$, 2.68 mmol/L $CaCl_2$, 5.26 mmol/L $NaHCO_3$, 10 mmol/L HEPES) for 1 h at 37°C, followed by incubation with either 0.5 or 3 mg/ml glucose for 30 min at 37°C. Insulin in media was measured using an ELISA kit (ALPCO) according to the manufacturer's protocol.

12) Statistical analysis

Statistical comparisons between the two groups were made using Student's two-tailed t-test or two-tailed paired t-test. One-way ANOVA with Tukey post hoc analysis using Prism™ 5 software (GraphPad, San Diego, CA) was applied when more than two groups were compared. Data are expressed as the mean ± standard deviation (SD).

4. Results and Conclusions

1) mtDNA mutations in iPSC clones derived from the blood of a 71-year-old type 2 diabetic patient

For subsequent studies, we used PBMC-derived iPSCs (BiPSCs) because BiPSCs were comparable to mtDNA mutations and blood is relatively easy to obtain compared with other tissues. The BiPSCs from T2D-2 patients from the previous chapter (T2D-2 BiPSCs) were selected (Table 2). All T2D-2 BiPSC clones showed normal PSC morphology (Figure 6A); however, mtDNA mutations in various regions such as RNA, syn, and non-syn, were detected in T2D-2 BiPSC clones that were not present in PBMCs. Notably, clones 2 and 3 showed the lowest heteroplasmy and had only RNA mutations, whereas non-syn mutations were observed in clones 1 and 4, and syn mutations were observed only in clone 5 (Figure 6B).

We calculated the sum of mtDNA mutations in the RNA and non-syn region to determine the risk of mutations in each iPSC clone (Figure 6C). It was highest in clone 1 at 113%, followed by clone 4 at 88%. We also investigated the mtDNA copy number in iPSC clones using qPCR (Figure 6D). Surprisingly, iPSC clone 1 exhibited a lower mtDNA copy number (617±124 copies) compared with the other clones ($p < 0.05$), which had a mt6678A>G mutation in the mitochondrially-encoded cytochrome oxidase subunit I (COI) gene with homoplasmy (100% heteroplasmy) and an mt7970G>A mutation in the mitochondrially-encoded cytochrome oxidase subunit II (COII) gene with 13% heteroplasmy. We analyzed the mtDNA copy number according to the heteroplasmy sum to confirm the association between the RNA and non-syn mutation and the mtDNA copy number (Figure 6E). As the heteroplasmy of RNA and non-syn mutations increased, the mtDNA copy number decreased but it was not significant ($p = 0.093$).

In summary, the morphology of iPSCs could not distinguish whether mtDNA mutations are present or not. However, mutations in functional positions could be correlated with the copy number of mtDNA.

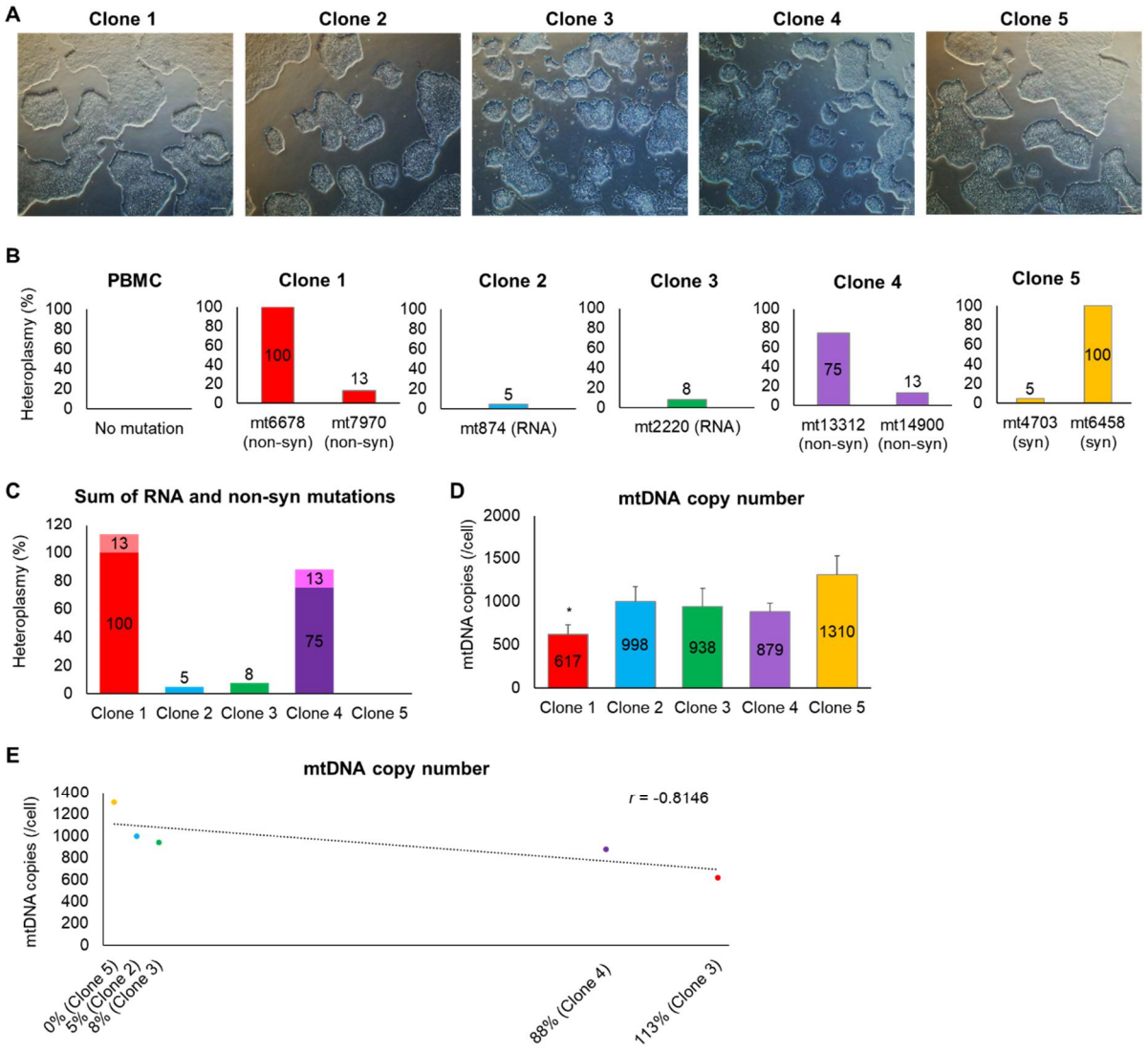

Figure 6. Displaying of mtDNA mutations in T2D-2 BiPSC clones. (A) Morphology of T2D-2 BiPSC clones. All iPSC clones showed normal morphology of the iPSC colonies. Scale bar = 100 μm. (B) mtDNA mutations and heteroplasmy in individual clones. (C) Total heteroplasmy of RNA and non-syn mutations in iPSCs. Clones 1 and 4 contained high heteroplasmy RNA and non-syn mutations. (D) mtDNA copy number in iPSC clones. mtDNA copy number of Clone 1 was lower than that of the other clones (*: $p < 0.05$, 3 technical replicates). (E) Distribution of mtDNA copy number according to the total heteroplasmy of RNA and non-syn mutations.

2) Differentiation to pancreatic progenitor cells from T2D-2 BiPSC lines

To determine the relationship between mtDNA mutations and pancreatic lineage differentiation, T2D-2 BiPSC clones were differentiated into pancreatic progenitor cells (PPCs) following a previously reported protocol (79). The represented PPC markers, including *PDX1, NGN3*, and *NKX6.1*, were analyzed in iPSC-derived PPCs by qRT-PCR (Figure 7A). The expression of these genes was significantly lower in clone 1-derived PPCs compared with the other clones ($p < 0.05$), except clone 4. Also, to determine the relationship between amino acid alterations by mtDNA mutation and the expression of PPC-related genes, we examined the expression of each gene according to the sum of the heteroplasmy of RNA mutations and non-syn mutations (Figure 7B). As the heterogeneity of the mtDNA mutant that changed the amino acid sequence increased, the expression of PPC-related genes except for *NKX6.1* ($p = 0.053$) showed a tendency to decrease significantly (*PDX1*; $p = 0.011$, *NGN3*; $p = 0.007$). To determine the relationship between mtDNA mutations and PPC markers at the protein level, the population of PDX1 protein-positive cells was determined by flow cytometry, which resulted in the lowest amount in clone 1 (39±18%, $p < 0.05$) (Figure 7C).

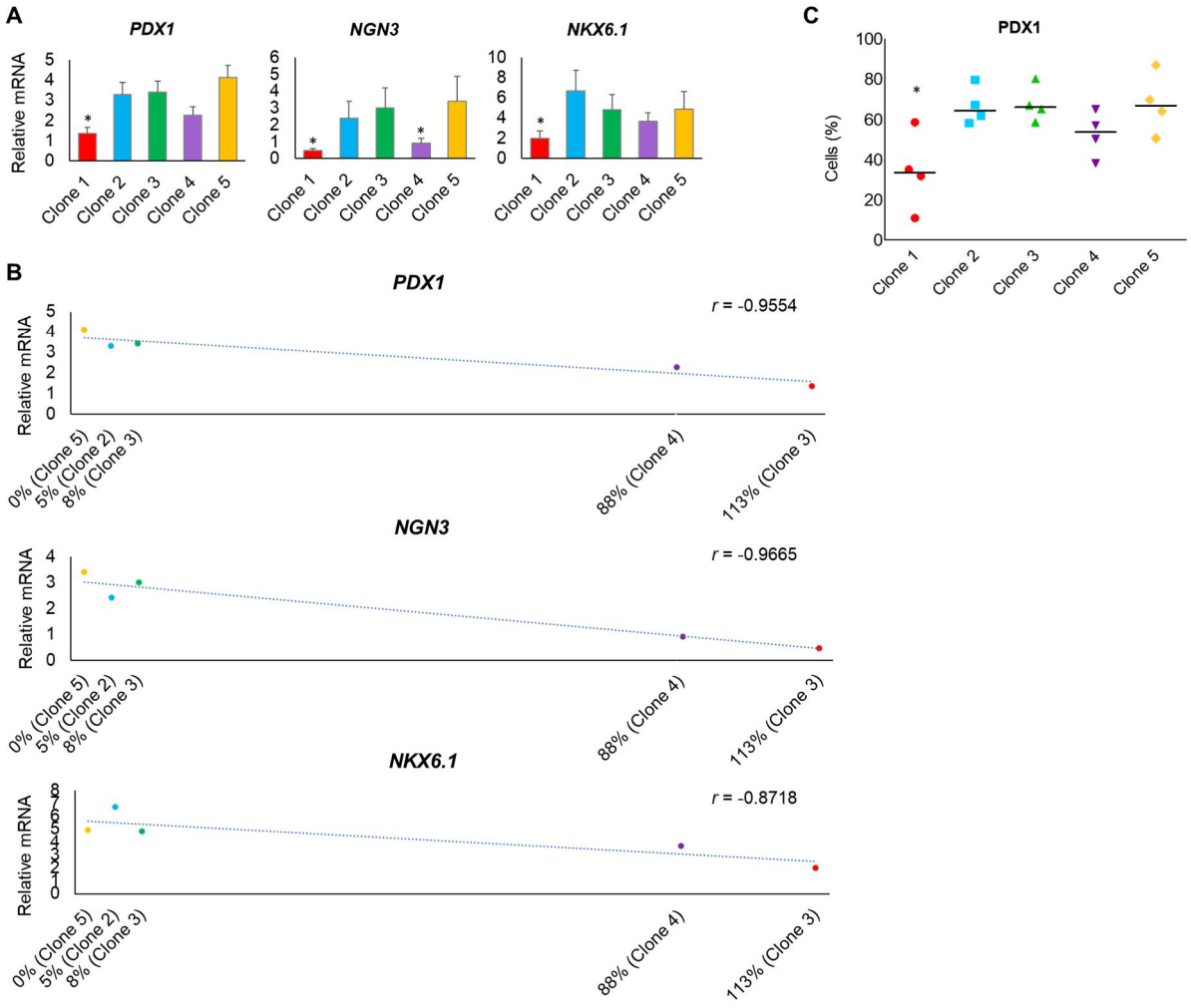

Figure 7. Pancreatic progenitor cells (PPCs) differentiated from T2D-2 BiPSCs. (A) Quantitative PCR analysis of the expression of PPC markers, *PDX1, NGN3*, and *NKX6.1*, relative to *GAPDH*. All PPC-related gene expression in clone 1 was significantly lower compared with that in other cell lines (*: $p < 0.05$, 2 biological replicates, 3 technical replicates). (B) PPC-related gene expression was inversely proportional to the sum of the heteroplasmy of mtDNA mutations in the positions of change of the amino acid, and RNA. As the mtDNA heteroplasmy increases, the expression of PPC-related genes decreases. (C) Flow cytometry analysis of PDX1 expression of PPCs derived from iPSCs. Clone 1-derived PPC had the lowest PDX1 positive population (*: $p < 0.05$, 4 biological replicates).

Finally, we investigated mitochondrial respiration function in iPSC clone 1 (mutant, non-syn mtDNA mutations with high heteroplasmy and low mtDNA copy number) and clone 2 (healthy, low heteroplasmy) with a seahorse platform. Clone 1-derived PPCs showed reduced oxygen consumption rates (OCR) compared with clone 2 (Figure 8A). Basal OCR, maximal respiration, ATP production, and spare respiratory capacity were significantly lower in clone 1 than in clone 2 (Figure 8B). These findings demonstrate that high heteroplasmic, non-synonymous mtDNA mutations may decrease PPC-related gene expression and mitochondrial respiratory function in PPCs.

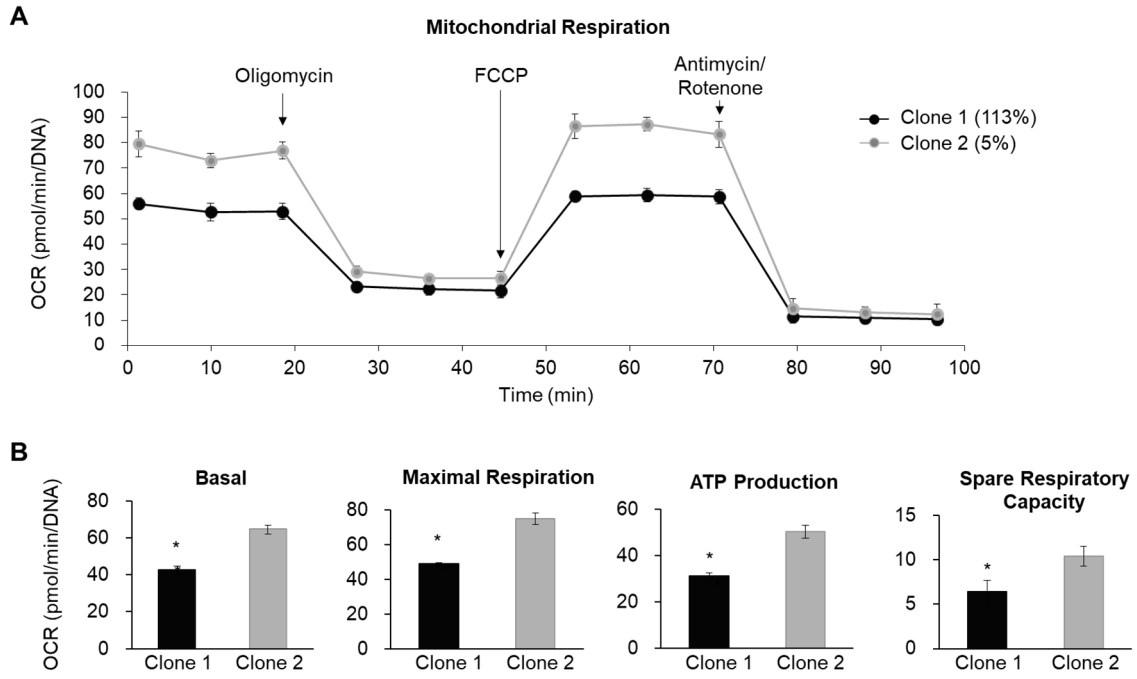

Figure 8. Mitochondrial dysfunction mediated by mtDNA mutations in pancreatic progenitor cells. (A) OCR levels in iPSC-derived PPCs. OCR levels in clone 1-derived PPCs were lower than those in clone 2. (B) Analysis of basal OCR, maximal respiration, ATP production, and spare respiratory capacity. In clone 1, all OCRs were significantly lower compared with clone 2 (*: $p < 0.05$, 3 technical replicates).

3) Effect of mtDNA mutations on pancreatic cell differentiation.

Based on the previous results, we performed pancreatic spheroid differentiation using PPCs derived from T2D-2 BiPSC clone 1 (mutant, non-syn mutations with high heteroplasmy, low PDX1 expression) and clone 2 (healthy, low heteroplasmy, normal PDX1 expression) to investigate whether the mtDNA mutations affected differentiation into pancreatic β-cells. There was no difference in the number (381/384 vs. 382/384) and size (77 vs. 80 μm) of the aggregates (Figure 9A, $p > 0.05$). Prior to the analysis of differentiated cells, we first analyzed copy number variations (CNVs) in clone 1 and clone 2 (Figure 9B). Both clones had the normal genotype (2N) in CNV analysis. We also investigated the mutations in the genomic DNA (gDNA) of differentiated pancreatic β-cells through exome sequencing in order to exclude the effect on the experiment due to the gDNA mutations. No mutations in gDNA were found in clone 1-derived β-cells, and exonic mutation was found in chromosomes 1q21.2 (*PLEKHO1*, Del) (Table 4). Although *PLEKHO1* has been reported to play a role in the regulation of the actin cytoskeleton, this gene has never been reported to be associated with PSC or pancreatic physiology, and the mutation frequency in whole cells was as low as 9%. Since we confirmed that there are no variables due to gDNA mutation, we next investigated the effect of mtDNA mutation on β-cell differentiation. The represented β-cell markers, including *INSULIN*, *PDX1*, and *NKX6.1*, were analyzed in iPSC clone 1- and 2-derived β-cells by qRT-PCR. All pancreatic β cell-related gene expressions were lower in clone 1 compared to clone 2, but both clones had lower gene expression than in human primary islets (Figure 9C, $p < 0.05$). Also, insulin synthesis was observed in pancreatic β-cells derived from both iPSC clones by immunocytochemistry (ICC) (Figure 9D). Most of the β-cells derived from clone 2 expressed insulin, whereas clone 1-derived β-cells showed little or no expression in some cells.

To determine whether mtDNA mutations were preserved after differentiation, we detected the mt6678A>G mutation, which was present in clone 1, in pancreatic cells derived from clones 1 and 2 using Sanger sequencing (Figure 9E). The results showed that this mutation was present at a rate of 100% in clone 1, but was completely absent in clone 2, suggesting that mtDNA mutations were retained during differentiation.

These results indicate that high heteroplasmic non-syn mtDNA mutations impair β-cell differentiation.

Table 4. Exome sequencing in β-cells derived from clone 1 and clone 2

Origin clone	Gene	Function	Locus	PSC and pancreatic association	Variant Type	Reference_Allele	Allele frequency (%)
Clone 1 (Mut)				ND			
Clone 2 (Wild)	*PLEKHO1*	Actin cytoskeleton regulation	1q21.2	-	Del	AACAGCCCGGTA ACACGGTATGTTT CTCCTGCC	9

*ND: not detected

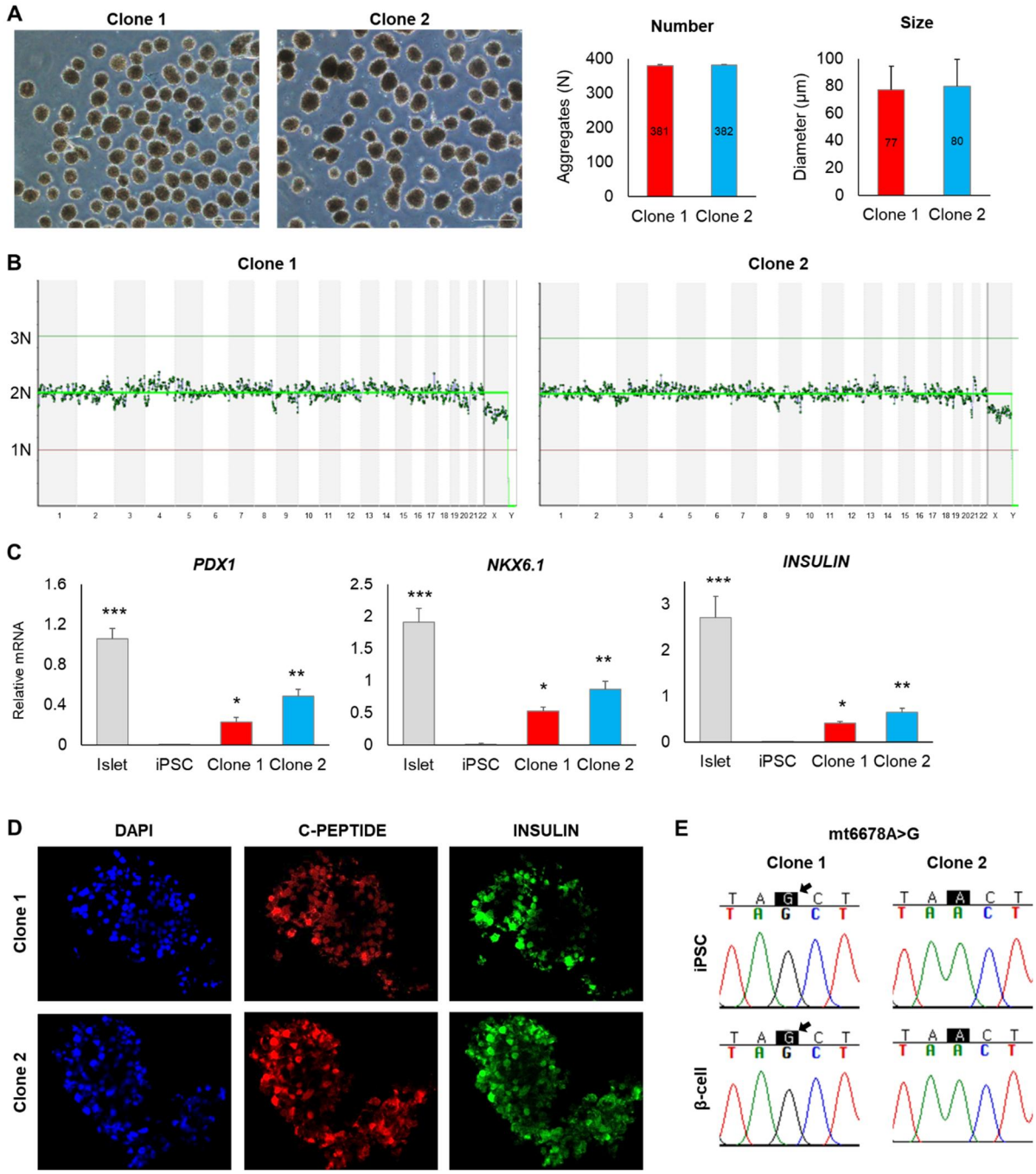

Figure 9. mtDNA mutations affect pancreatic β-cell differentiation. (A) Pancreatic β-cell aggregates derived from clones 1 and 2. Both clones showed similar aggregate formation. Scale bar = 200 μm (B) Copy number variations (CNVs) analysis using Veriseq platform in clones 1 and 2. Both clones showed normal CNV. (C) Quantitative RT-PCR analysis of β-cell marker expressions including, *PDX1*, *NKX6.1*, and *INS* relative to *GAPDH*. Clone 1-derived β-cells had lower β cell-related gene expression compared with clone 2. β-cells derived from both clones showed lower expression of all genes compared to human

islets. (*: $p < 0.05$, 2 biological, 3 technical replicates). (D) Immunocytochemistry examining the C-PEPTIDE (red) and INSULIN (green) expression of β-cells. Nuclei were stained with DAPI (blue). Scale bar = 20 μm (E) Sanger sequencing of iPSC clones 1 and 2 and the β-cells derived from them. The mt6678A>G mutation in clone 1 was preserved after β-cell differentiation. Black arrows indicate the mtDNA mutation chromatography peak.

4) mtDNA mutation-mediated abnormal metabolism in pancreatic β-cells

First, we analyzed the metabolites of iPSC-derived β cells to investigate the effects of mtDNA mutations on metabolic processes (Figure 10A-C). The amount of glucose (GLC) in clone 1 β-cells was only slightly lower compared with that in their clone 2 counterparts. In contrast, glucose-6-phosphate and fructose-6-phosphate (G6P/F6P) were significantly lower in clone 1. Glucose is converted to F6P via G6P during glycolysis (Figure 10A, $p < 0.05$). Among the metabolites related to the TCA cycle, the amount of malate (MAL) and nicotinamide adenine dinucleotide (NAD) was significantly higher in clone 2 derived β-cells (Figure 10B, $p < 0.05$). Taken together, the mtDNA mutation appears to decrease the overall ATP production by reducing the glycolysis of glucose in β-cells and inhibiting the production of MAL, a late product in the TCA cycle in mitochondria. During this process, NAD is also reduced by mtDNA mutations, which are thought to cause abnormal metabolism (Figure 10C).

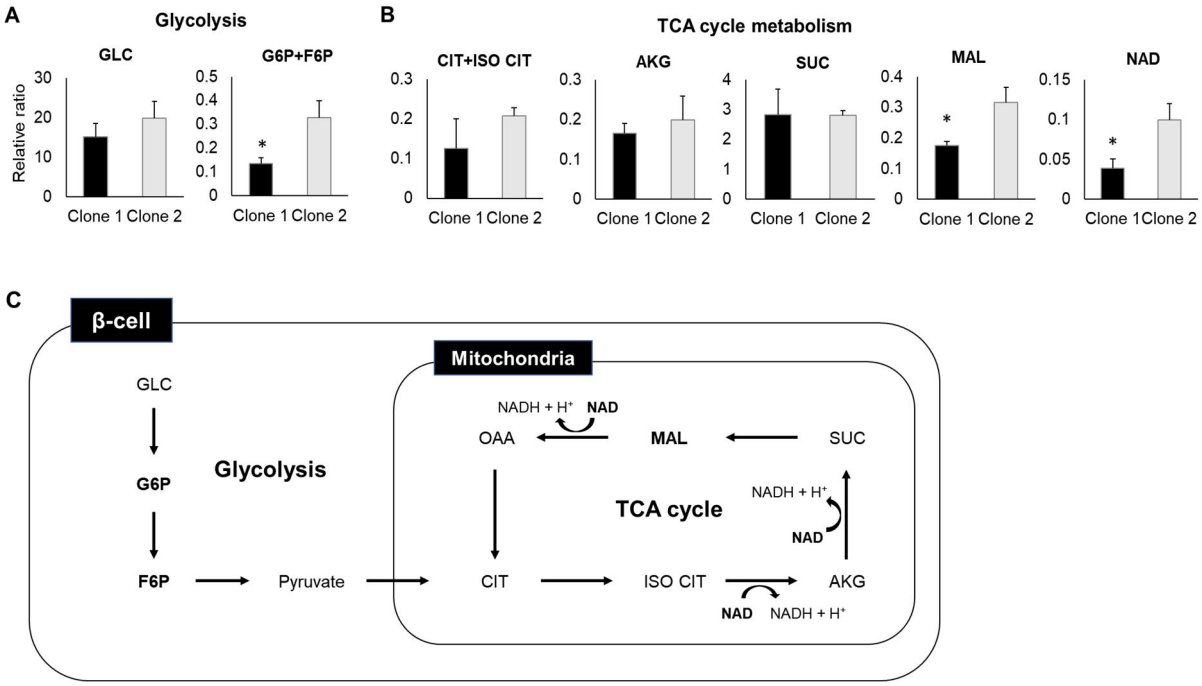

Figure 10. Metabolic decline by mtDNA mutations in pancreatic β-cells. (A) Comparison of glycolysis-related metabolites in β-cells derived from clones 1 and 2. There was no difference in GLC between groups, however, G6P and F6P were lower in clone 1. (B) TCA cycle-related metabolite analysis. MAL and NAD were higher in β-cells derived from clone 2 compared with clone 1 (*: p <0.05, 3 biological replicates). (C) Glucose metabolism in β-cells. Bold text indicates metabolites reduced by mtDNA mutation.

5) Pancreatic dysfunction caused by mtDNA mutations

Next, we investigated the insulin content of β-cells derived from T2D-2 BiPSC clones 1 and 2 to determine the effect of mtDNA mutations on insulin production (Figure 11A). Intracellular insulin was significantly lower in clone 1 than in clone 2. To examine the effect of mtDNA mutation on the insulin-secreting function of β-cells, glucose-stimulated insulin secretion (GSIS) was induced by low and high glucose treatment of iPSC-derived β cells (Figure 11B) (80). Normal β-cells secrete low insulin under low glucose conditions and increased insulin secretion when the glucose concentration increases (81). Clone 1-derived β-cells exhibited low levels of insulin secretion at low glucose concentrations but did not increase insulin secretion even when the glucose concentration was increased, whereas clone 2 significantly increased insulin secretion at high glucose concentrations ($p < 0.05$). These results indicate that high heteroplasmic non-syn mtDNA mutations can cause problems in metabolic processes and affect insulin production and insulin-secreting function in β-cells.

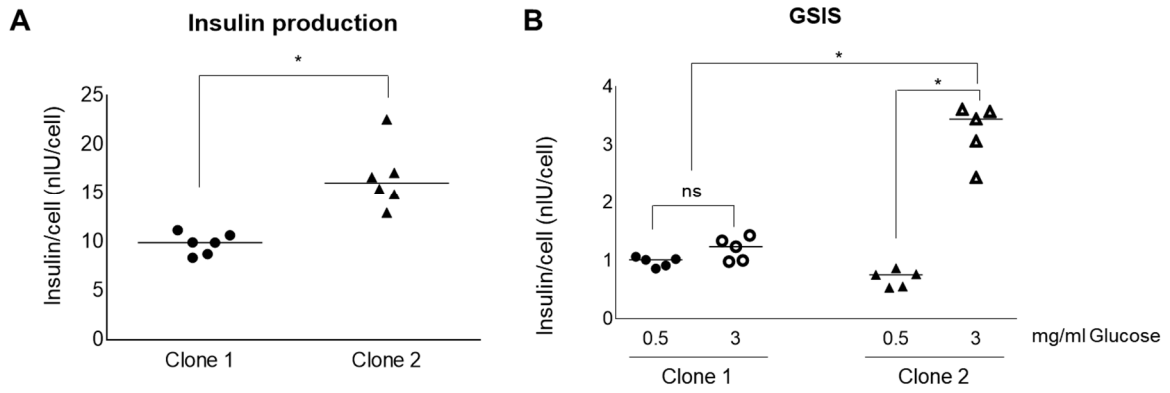

Figure 11. mtDNA mutations reduce insulin production and secretion. (A) Insulin content in β-cells derived from iPSC clones. The insulin of pancreatic β-cells derived from clone 2 was significantly higher than that of clone 1 (*: $p < 0.05$, 6 replicates). (B) GSIS analysis of pancreatic β-cells derived from iPSC clones. Clone 2-derived pancreatic β-cells cells increased the amount of insulin secretion when glucose concentration increased, whereas clone 1-derived pancreatic β-cells did not (*: $p < 0.05$, 5 replicates).

In summary, our study showed that mtDNA mutations are found randomly after iPSC induction and can reduce pancreatic lineage differentiation. We also demonstrated that mtDNA mutations can impair metabolism and cause abnormalities in insulin production and secretion after pancreatic β-cell differentiation (Figure 12).

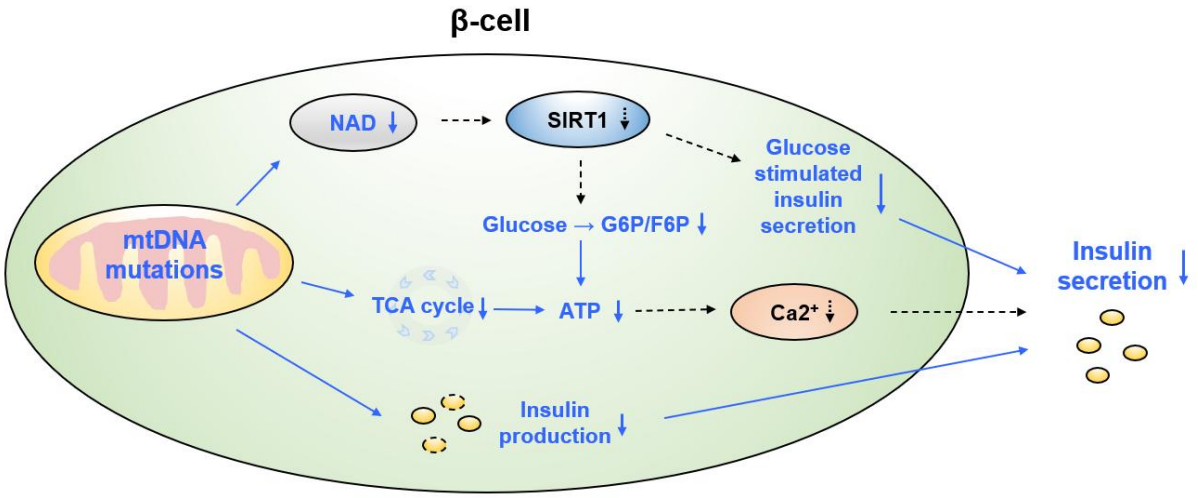

Figure 12. Schematic summary of the insulin secretion inhibition pathway by mtDNA mutations. mtDNA mutations can inhibit insulin secretion in three major ways. First, SIRT1 is inactivated by inhibiting the production of NAD. Second, ATP production is lowered because of the abnormality of the TCA cycle. Finally, mutations may inhibit a pathway that suppresses the production of insulin. Blue text and line = analyzed in this study, Black text and dotted line = reported in the previous study.

[Chapter III was prepared based on [BMB-22-023] Dysfunctional pancreatic cells differentiated from induced pluripotent stem cells with mitochondrial DNA mutations.]

Chapter IV.

Conclusions

In this thesis, we established iPSCs in type 2 diabetes patients and tried to study the tendency of mtDNA mutations and the abnormalities in the derived pancreatic cells. Before entering this study, we first established a method for efficiently culturing iPSCs in Chapter II. Y-27632, a ROCK inhibitor used by many researchers, is more expensive than other ROCK inhibitors because the synthesis process is complicated and has isomers. Therefore, we tried to determine the effectiveness and safety of using fasudil, a low-cost ROCK inhibitor that has been clinically approved in many countries, instead of Y-27632. Fasudil increased the growth of PSCs similarly to Y-27632 and did not affect the pluripotency, karyotype, and differentiation capacity of PSCs despite long-term culture. These results show that xeno-free PSC culture that is safe and effective for growth is possible by treating fasudil.

Based on the PSC culture method demonstrated in Chapter II, we established and cultured iPSCs from 3 type 2 diabetic patients in Chapter III-1. Then, the mtDNA of somatic cells and iPSCs was analyzed through mtDNA sequencing. As a result of analyzing the mtDNA mutations of iPSCs of 3 diabetic patients, no diabetes-specific mtDNA mutations were found, and there was no significant difference in the number of mtDNA mutations of iPSCs derived from fibroblasts, PBMCs, and pancreatic cells. Interestingly, more homoplasmic mtDNA mutations were found in iPSCs of diabetic patients when mtDNA mutations in iPSCs of non-diabetic and diabetic patients were analyzed, and the heteroplasmy of total mutations was also higher in diabetic patients. This suggests that the presence of pathological mtDNA mutations in iPSCs may be higher when iPSCs are established from diabetic patients and used for cell therapy or research.

In Chapter III-2, based on previous results, we investigated how pathologic mtDNA mutation with high heteroplasmy affects iPSC differentiation into pancreatic cells and post-differentiation function. iPSC clones derived from one type 2 diabetic patient were selected and differentiated into pancreatic cells. As a result of examining gene expression and protein expression in pancreatic progenitor cells, the higher the sum of heteroplasmy of non-syn mutations that change the amino acid sequence and mutations that exist at the RNA coding region, the tendency for pancreatic development-related gene expression to decrease. Clone 1 with the homoplasmic mtDNA mutation also had a low proportion of cells expressing PDX1, a protein related to pancreatic development. Based on this, we differentiated wild-type and mutant clones with low expression of pancreatic development-related genes and proteins into pancreatic β-cells. Gene expression in pancreatic β-cells was lower in the mutants and mtDNA mutations did not change after differentiation. As a result of the analysis of glycolysis and TCA cycle-related metabolism after differentiation, it was confirmed that metabolites

such as G6P, F6P, malate, and NAD were decreased in the mutant. Insulin production was also lower in the mutant compared with the wild-type clone, and the function of secreting insulin in response to glucose did not function normally in the mutant. These data show that mtDNA mutations with high heteroplasmy, which are often found in iPSCs derived from diabetic patients, may affect pancreatic differentiation, and have the potential to cause dysfunction of differentiated pancreatic cells, so it is essential to analyze mtDNA mutations after the establishment of iPSCs from diabetic patients.

Chapter V.

Discussion

It has been reported that iPSC clones derived from the same individual harbored different somatic mtDNA mutations. Mitochondrial DNA mutations may affect the differentiation of iPSCs into target cells such as neural cells, cardiomyocytes, and fibroblasts (19, 82-85). Like the mt3243A>G mutation, there are well-known mtDNA mutations that are closely related to DM (86), however, to our knowledge, there are no reports of the effects of somatic mtDNA mutations on the differentiation of pancreatic cells from iPSCs and their function. The mitochondrial genome is closely related to ATP production in mitochondria and the insulin secretion of pancreatic β-cells is regulated by ATP generated by externally absorbed glucose (87, 88). Regulating insulin secretion in pancreatic β-cells is important for glucose homeostasis (89). In diabetic patients, the postprandial glucose-stimulated insulin secretion (GSIS) is insufficient in β-cells, which is characteristic of diabetic pathology (90). Although the molecular mechanisms involved in GSIS are well known, the correlation between mtDNA mutations and GSIS is unclear and requires further exploration.

In this study, we analyzed mtDNA mutations in iPSCs derived from fibroblasts, PBMCs, and pancreatic cells from every 3 T2D patients and 3 ND patients. We found no clear association between specific mtDNA mutations and tissue or T2D disease. According to a previous report, the novel mutations are only observed in iPSC lines derived from origin cells that were not generated by reprogramming (19, 91). Similarly, we revealed that individual iPSC clones derived from T2D patients have different mtDNA mutations, and all of the mtDNA mutations identified in iPSC clones were not present in the pooled parental cells. Interestingly, the mt10535T>C mutation with more than 50% heteroplasmy was found to occur frequently in blood and pancreatic cells derived from T2D-3 patients, but not in all iPSCs derived from the T2D-3 patient. This may result from a negative selection of the mt10535T>C mutation during iPSC induction.

A high proportion (61%) of iPSCs derived from T2D patients exhibited mtDNA mutations and more than half (55%) of the mutations in iPSCs contained more than 50% heteroplasmy. In addition, homoplasmic mtDNA mutations were found more frequently in iPSCs from patients with T2D compared to ND. These results suggest that it is essential to screen for mtDNA mutations when using iPSCs for patient-specific research and treatment.

Next, we selected iPSC lines derived from the blood of a 71-year-old T2D-2 patient and analyzed the morphology and mtDNA copy number of each clone. All iPSC clones with or without mtDNA mutations had normal PSC morphology; however, for iPSC clone 1 with high heteroplasmic non-syn mtDNA mutation, the mtDNA copy number was significantly lower compared with other

clones, suggesting that the mtDNA copy number may be another indicator of the safety for differentiation (92).

Currently, islet transplantation is being performed worldwide to treat diabetes, but many patients are waiting for surgery due to a shortage of supplies. T2D requires islet transplantation in severe cases, and as shown in the transplant results of *Choi et al* (93), it can be seen that 20% of all islet transplant patients were T2D patients. To investigate the effect of mtDNA mutations when using iPSCs as autologous cell therapy for T2D, we differentiated iPSC clones into pancreatic lineage cells. We demonstrated that high heteroplasmic mtDNA mutations negatively affected the expression of several pancreatic-specific genes including *PDX1*, *NKX6.1*, and *NGN3*. PDX1 expression, in particular, is very important for β-cell development and the regulation of insulin secretion from pancreatic β-cells (94). As such, iPSC clone 1 (mutant), with low PDX1 expression after β-cell differentiation, showed lower insulin expression compared with normal clones and failed to increase insulin secretion in response to high glucose concentration. In the mitochondrial respiration assay, the ATP production capacity of clone 1 was lower than that of the normal clone, suggesting that the mtDNA mutation impaired ATP production, which, in turn, affected ATP-dependent insulin secretion (95, 96). During metabolite analysis, the intracellular NAD content was significantly lower in clone 1. NAD is essential for cellular redox reactions in all living organisms and low levels of NAD in β-cells may decrease the activity of SIRT1, which may lead to abnormal insulin secretion (97, 98). In addition, it has been reported that when a mitochondrial respiratory deficiency occurs, NAD is suppressed and the activity of SIRT is concomitantly reduced (99). G6P and F6P were also lower in clone 1-derived β-cells (Figure 10) and studies have reported that SIRT1 downregulation inhibits the conversion of glucose to G6P and F6P in β-cells (98, 100).

Since only 3 diabetic patients analyzed mtDNA mutations in iPSCs, there is a limitation that a larger-scale analysis is needed in the future. In addition, since the differentiation analysis of iPSCs derived from diabetic patients was only one, there is a limit to the need for a study on whether mtDNA mutations have different effects depending on the mutant locus. Despite these limitations, our study demonstrated that more homoplasmic mtDNA mutations are found in type 2 diabetic patients and these mtDNA mutations have the potential to impair the differentiation and function of pancreatic cells. This suggests that screening the mtDNA is essential prior to further research for disease modeling and clinical application of iPSCs as autologous cell therapies. In a further study, we will select other iPSC clones with different mtDNA mutations derived from diabetic patients, differentiate them into pancreatic cells,

and analyze their dysfunction.

Chapter VI.

References

1. Egan AM and Dinneen SF (2019) What is diabetes? Medicine. 47, 1-4
2. Ozougwu J, Obimba K, Belonwu C and Unakalamba C (2013) The pathogenesis and pathophysiology of type 1 and type 2 diabetes mellitus. Journal of Physiology and Pathophysiology 4, 46-57
3. Kondo Y, Toyoda T, Inagaki N and Osafune K (2018) iPSC technology based regenerative therapy for diabetes. Journal of Diabetes Investigation 9, 234-243
4. Kim MJ, Lee EY, You Y-H, Yang HK, Yoon K-H and Kim J-W (2020) Generation of iPSC-derived insulin-producing cells from patients with type 1 and type 2 diabetes compared with healthy control. Stem Cell Research 48, 101958
5. Shahjalal HM, Abdal Dayem A, Lim KM, Jeon T-i, Cho S-G (2018) Generation of pancreatic β cells for treatment of diabetes: advances and challenges. Stem cell research therapy 9, 1-19
6. Takahashi K, Tanabe K, Ohnuki M et al (2007) Induction of pluripotent stem cells from adult human fibroblasts by defined factors. Cell 131, 861-872
7. Kurosawa H (2012) Application of Rho-associated protein kinase (ROCK) inhibitor to human pluripotent stem cells. Journal of bioscience and bioengineering 114, 577-581
8. Jozefczuk J, Drews K and Adjaye J (2012) Preparation of mouse embryonic fibroblast cells suitable for culturing human embryonic and induced pluripotent stem cells. Journal of Visualized Experiments e3854
9. Watanabe K, Ueno M, Kamiya D et al (2007) A ROCK inhibitor permits survival of dissociated human embryonic stem cells. Nature biotechnology 25, 681-686
10. So S, Lee Y, Choi J et al (2020) The Rho-associated kinase inhibitor fasudil can replace Y-27632 for use in human pluripotent stem cell research. PloS one 15, e0233057
11. Greaves LC, Reeve AK, Taylor RW and Turnbull DM (2012) Mitochondrial DNA and disease. The Journal of Pathology 226, 274-286
12. Taylor RW and Turnbull DM (2005) Mitochondrial DNA mutations in human disease. Nature Reviews Genetics 6, 389-402
13. Tseng LM, Yin PH, Chi CW et al (2006) Mitochondrial DNA mutations and mitochondrial DNA depletion in breast cancer. Genes, Chromosomes Cancer 45, 629-638
14. Gorman GS, Schaefer AM, Ng Y et al (2015) Prevalence of nuclear and mitochondrial DNA mutations related to adult mitochondrial disease. Annals of Neurology 77, 753-759
15. Kwak SH, Park KS, Lee KU and Lee HK (2010) Mitochondrial metabolism and diabetes. Journal of diabetes investigation 1, 161-169
16. JI L, HOU X and HAN X (2001) Prevalence and clinical characteristics of mitochondrial tRNA leu (UUR) mt 3243 A→ G and ND-1 gene mt 3316 G→ A mutations in Chinese patients with type 2 diabetes. Chinese Medical Journal 114, 1205-1207
17. Larsson N-G (2010) Somatic mitochondrial DNA mutations in mammalian aging. Annual review of

biochemistry 79, 683-706

18. Kang E, Wang X, Tippner-Hedges R et al (2016) Age-related accumulation of somatic mitochondrial DNA mutations in adult-derived human iPSCs. Cell stem cell 18, 625-636
19. Trifunovic A, Wredenberg A, Falkenberg M et al (2004) Premature ageing in mice expressing defective mitochondrial DNA polymerase. Nature 429, 417-423
20. McNeish J (2004) Embryonic stem cells in drug discovery. Nature Reviews Drug Discovery 3, 70-80
21. Carpenter MK and Rao MS (2015) Concise review: making and using clinically compliant pluripotent stem cell lines. Stem cells translational medicine 4, 381-388
22. Ilic D and Ogilvie C (2017) Concise review: Human embryonic stem cells—what have we done? What are we doing? Where are we going? Stem Cells 35, 17-25
23. Thomson JA, Itskovitz-Eldor J, Shapiro SS et al (1998) Embryonic stem cell lines derived from human blastocysts. Science 282, 1145-1147
24. Ludwig TE, Levenstein ME, Jones JM et al (2006) Derivation of human embryonic stem cells in defined conditions. Nature biotechnology 24, 185
25. Richards M, Fong C-Y, Chan W-K, Wong P-C and Bongso A (2002) Human feeders support prolonged undifferentiated growth of human inner cell masses and embryonic stem cells. Nature biotechnology 20, 933-936
26. Reubinoff BE, Pera MF, Fong C-Y, Trounson A and Bongso A (2000) Embryonic stem cell lines from human blastocysts: somatic differentiation in vitro. Nature biotechnology 18, 399-404
27. Mallon BS, Park K-Y, Chen KG, Hamilton RS and McKay RD (2006) Toward xeno-free culture of human embryonic stem cells. The international journal of biochemistry & cell biology 38, 1063-1075
28. Dravid G, Ye Z, Hammond H et al (2005) Defining the role of Wnt/β catenin signaling in the survival, proliferation, and self renewal of human embryonic stem cells. Stem cells 23, 1489-1501
29. Villa Diaz L, Ross A, Lahann J and Krebsbach P (2013) Concise review: the evolution of human pluripotent stem cell culture: from feeder cells to synthetic coatings. Stem cells 31, 1-7
30. Hasegawa K, Yasuda S-y, Teo J-L et al (2012) Wnt signaling orchestration with a small molecule DYRK inhibitor provides long term xeno free human pluripotent cell expansion. Stem cells translational medicine 1, 18-28
31. Huang SX, Islam MN, O'neill J et al (2014) Efficient generation of lung and airway epithelial cells from human pluripotent stem cells. Nature biotechnology 32, 84
32. Rezania A, Bruin JE, Arora P et al (2014) Reversal of diabetes with insulin-producing cells derived in vitro from human pluripotent stem cells. Nature biotechnology 32, 1121
33. Braam SR, Tertoolen L, van de Stolpe A, Meyer T, Passier R and Mummery CL (2010) Prediction of drug-induced cardiotoxicity using human embryonic stem cell-derived cardiomyocytes. Stem cell research 4, 107-116

34. Higuchi A, Kumar SS, Ling Q-D et al (2017) Polymeric design of cell culture materials that guide the differentiation of human pluripotent stem cells. Progress in Polymer Science 65, 83-126
35. Osakada F, Jin Z-B, Hirami Y et al (2009) In vitro differentiation of retinal cells from human pluripotent stem cells by small-molecule induction. Journal of cell science 122, 3169-3179
36. Ohgushi M, Matsumura M, Eiraku M et al (2010) Molecular pathway and cell state responsible for dissociation-induced apoptosis in human pluripotent stem cells. Cell stem cell 7, 225-239
37. Paleček J, Zweigerdt R, Olmer R, Martin U, Kirschning A and Dräger G (2011) A practical synthesis of Rho-Kinase inhibitor Y-27632 and fluoro derivatives and their evaluation in human pluripotent stem cells. Organic & biomolecular chemistry 9, 5503-5510
38. Feng Y, LoGrasso PV, Defert O and Li R (2016) Rho kinase (ROCK) inhibitors and their therapeutic potential. Journal of medicinal chemistry 59, 2269-2300
39. YAO J-w, WANG C-p, ZHANG X-j and XU W-f (2012) Synthesis of fasudil hydrochloride. 3
40. Nie Y, Walsh P, Clarke DL, Rowley JA and Fellner TJPo (2014) Scalable passaging of adherent human pluripotent stem cells. PloS one 9, e88012
41. Wu J, Fan Y and Tzanakakis ES (2015) Increased culture density is linked to decelerated proliferation, prolonged G1 phase, and enhanced propensity for differentiation of self-renewing human pluripotent stem cells. Stem cells and development 24, 892-903
42. Totsukawa G, Wu Y, Sasaki Y et al (2004) Distinct roles of MLCK and ROCK in the regulation of membrane protrusions and focal adhesion dynamics during cell migration of fibroblasts. The Journal of cell biology 164, 427-439
43. Harb N, Archer TK and Sato N (2008) The Rho-Rock-Myosin signaling axis determines cell-cell integrity of self-renewing pluripotent stem cells. PloS one 3, e3001
44. Chen S, Luo M, Zhao Y et al (2015) Fasudil stimulates neurite outgrowth and promotes differentiation in C17. 2 neural stem cells by modulating notch signalling but not autophagy. Cellular Physiology and Biochemistry 36, 531-541
45. Ying H, Biroc SL, Li W-w et al (2006) The Rho kinase inhibitor fasudil inhibits tumor progression in human and rat tumor models. Molecular cancer therapeutics 5, 2158-2164
46. Meng Y, Ren Z, Xu F et al (2018) Nicotinamide Promotes Cell Survival and Differentiation as Kinase Inhibitor in Human Pluripotent Stem Cells. Stem cell reports 11, 1347-1356
47. Busche S, Descot A, Julien S, Genth H and Posern G (2008) Epithelial cell-cell contacts regulate SRF-mediated transcription via Rac-actin-MAL signalling. Journal of cell science 121, 1025-1035
48. Vigil D, Kim TY, Plachco A et al (2012) ROCK1 and ROCK2 are required for non-small cell lung cancer anchorage-independent growth and invasion. Cancer research 72, 5338-5347
49. Zhang J-G, Li X-Y, Wang Y-Z et al (2014) ROCK is involved in vasculogenic mimicry formation in hepatocellular carcinoma cell line. PloS one 9

50. Vicente-Manzanares M, Koach MA, Whitmore L, Lamers ML and Horwitz AF (2008) Segregation and activation of myosin IIB creates a rear in migrating cells. The Journal of cell biology 183, 543-554
51. Chinnery P, Mowbray C, Patel S et al (2007) Mitochondrial DNA haplogroups and type 2 diabetes: a study of 897 cases and 1010 controls. Journal of medical genetics 44, e80-e80
52. Mather H, Nisbet JA, Burton G et al (1979) Hypomagnesaemia in diabetes. Archives of medical research 95, 235-242
53. Caballero AE (2005) Metabolic and vascular abnormalities in subjects at risk for type 2 diabetes: the early start of a dangerous situation. Archives of medical research 36, 241-249
54. Mellitus D (2005) Diagnosis and classification of diabetes mellitus. Diabetes care 28, S5-S10
55. Lebovitz HE (1999) Type 2 diabetes: an overview. Clinical chemistry 45, 1339-1345
56. Leahy JL (2005) Pathogenesis of type 2 diabetes mellitus. Archives of medical research 36, 197-209
57. Robertson RP, Zhou H, Zhang T and Harmon JS (2007) Chronic oxidative stress as a mechanism for glucose toxicity of the beta cell in type 2 diabetes. Cell biochemistry and biophysics 48, 139-146
58. Kieffer TJ, Woltjen K, Osafune K, Yabe D and Inagaki N (2018) Beta cell replacement strategies for diabetes. Journal of diabetes investigation 9, 457-463
59. Suchy F, Yamaguchi T and Nakauchi H (2018) iPSC-derived organs in vivo: challenges and promise. Cell Stem Cell 22, 21-24
60. Nakagawa M, Koyanagi M, Tanabe K et al (2008) Generation of induced pluripotent stem cells without Myc from mouse and human fibroblasts. Nature biotechnology 26, 101-106
61. Okano H, Nakamura M, Yoshida K et al (2013) Steps toward safe cell therapy using induced pluripotent stem cells. Circulation research 112, 523-533
62. Park J, Lee Y, Shin J et al (2019) Mitochondrial genome mutations in mesenchymal stem cells derived from human dental induced pluripotent stem cells. BMB reports 52, 689
63. Reardon W, Pembrey M, Trembath R et al (1992) Diabetes mellitus associated with a pathogenic point mutation in mitochondrial DNA. The Lancet 340, 1376-1379
64. Park CB and Larsson N-G (2011) Mitochondrial DNA mutations in disease and aging. Journal of cell biology 193, 809-818
65. Wallace DC (1994) Mitochondrial DNA sequence variation in human evolution and disease. Proceedings of the National Academy of Sciences 91, 8739-8746
66. Zapico SC, Ubelaker DH (2013) mtDNA mutations and their role in aging, diseases and forensic sciences. Aging disease 4, 364
67. Reardon W, Pembrey M, Trembath R et al (1992) Diabetes mellitus associated with a pathogenic point mutation in mitochondrial DNA. The Lancet 340, 1376-1379
68. Ma H, Folmes CD, Wu J et al (2015) Metabolic rescue in pluripotent cells from patients with mtDNA disease. Nature 524, 234

69. Lee Y, Lee S-M, Choi J et al (2021) Mitochondrial DNA Haplogroup Related to the Prevalence of Helicobacter pylori. Cells 10, 2482
70. Ye K, Lu J, Ma F, Keinan A and Gu Z (2014) Extensive pathogenicity of mitochondrial heteroplasmy in healthy human individuals. Proceedings of the National Academy of Sciences 111, 10654-10659
71. Gorman GS, Chinnery PF, DiMauro S et al (2016) Mitochondrial diseases. Nature reviews disease primers 2, 1-22
72. Maechler P and Wollheim CB (2001) Mitochondrial function in normal and diabetic β-cells. Nature 414, 807-812
73. Park SW, Goodpaster BH, Strotmeyer ES et al (2006) Decreased muscle strength and quality in older adults with type 2 diabetes: the health, aging, and body composition study. Diabetes 55, 1813-1818
74. Ryan CMJNoa (2005) Diabetes, aging, and cognitive decline. Neurobiology of aging 26, 21-25
75. Kunisada Y, Tsubooka-Yamazoe N, Shoji M and Hosoya M (2012) Small molecules induce efficient differentiation into insulin-producing cells from human induced pluripotent stem cells. Stem cell research 8, 274-284
76. Eshaghian A, Vleugels RA, Canter JA, McDonald MA, Stasko T and Sligh JE (2006) Mitochondrial DNA deletions serve as biomarkers of aging in the skin, but are typically absent in nonmelanoma skin cancers. Journal of investigative dermatology 126, 336-344
77. Lee HY, Nam S, Kim MJ, Kim SJ, Back SH and Yoo HJ (2021) Butyrate Prevents TGF-β1-Induced Alveolar Myofibroblast Differentiation and Modulates Energy Metabolism. Metabolites 11, 258
78. Kunisada Y, Tsubooka-Yamazoe N, Shoji M and Hosoya M (2012) Small molecules induce efficient differentiation into insulin-producing cells from human induced pluripotent stem cells. Stem cell research 8, 274-284
79. Plecitá-Hlavatá L, Jabůrek M, Holendová B et al (2020) Glucose-Stimulated Insulin Secretion Fundamentally Requires H2O2 Signaling by NADPH Oxidase 4. Diabetes 69.7, 1341-1354.
80. MacDonald PE, El-kholy W, Riedel MJ, Salapatek AMF, Light PE and Wheeler MB (2002) The multiple actions of GLP-1 on the process of glucose-stimulated insulin secretion. Diabetes 51, S434-S442
81. Rossignol R, Faustin B, Rocher C, Malgat M, Mazat J-P and Letellier T (2003) Mitochondrial threshold effects. Biochemical journal 370, 751-762
82. Hatakeyama H and Goto Yi (2016) Concise review: heteroplasmic mitochondrial DNA mutations and mitochondrial diseases: toward iPSC based disease modeling, drug discovery, and regenerative therapeutics. Stem Cells 34, 801-808
83. Li S, Pan H, Tan C et al (2018) Mitochondrial dysfunctions contribute to hypertrophic cardiomyopathy in patient iPSC-derived cardiomyocytes with MT-RNR2 mutation. Stem cell reports 10, 808-821
84. Hämäläinen RH, Manninen T, Koivumäki H, Kislin M, Otonkoski T and Suomalainen A (2013) Tissue- and cell-type–specific manifestations of heteroplasmic mtDNA 3243A> G mutation in human induced

pluripotent stem cell-derived disease model. PNAS 110, E3622-E3630

85. Suzuki Y, Muramatsu T, Taniyama M et al (1996) Mitochondrial aldehyde dehydrogenase in diabetes associated with mitochondrial tRNALeu (UUR) mutation at position 3243. Diabetes care 19, 1423-1425

86. Kieffer TJ, Heller RS, Leech CA, Holz GG and Habener JF (1997) Leptin suppression of insulin secretion by the activation of ATP-sensitive K+ channels in pancreatic β-cells. Diabetes 46, 1087-1093

87. Rocheleau JV, Remedi MS, Granada B et al (2006) Critical role of gap junction coupled K ATP channel activity for regulated insulin secretion. Plos biology 4, e26

88. Rorsman P and Braun M (2013) Regulation of insulin secretion in human pancreatic islets. Annual review of physiology 75, 155-179

89. Kristinsson H, Smith DM, Bergsten P and Sargsyan E (2013) FFAR1 is involved in both the acute and chronic effects of palmitate on insulin secretion. Endocrinology 154, 4078-4088

90. Perrera V, Martello G (2019) How does reprogramming to pluripotency affect genomic imprinting? Frontiers in cell developmental biology 7, 76

91. Filograna R, Koolmeister C, Upadhyay M et al (2019) Modulation of mtDNA copy number ameliorates the pathological consequences of a heteroplasmic mtDNA mutation in the mouse. Science advances 5, eaav9824

92. Choi JY, Jung JH, Shin S, Kim YH and Han DJ (2017) Association between the pancreas transplantation and survival of patients with diabetes: A single center experience. PLoS One 12, e0186827

93. Gauthier BR, Wiederkehr A, Baquié M et al (2009) PDX1 deficiency causes mitochondrial dysfunction and defective insulin secretion through TFAM suppression. Cell metabolism 10, 110-118

94. Shepherd R, Checcarelli N, Naini A, De Vivo D, DiMauro S and Sue C (2006) Measurement of ATP production in mitochondrial disorders. Journal of Inherited Metabolic Disease 29, 86-91

95. Kennedy ED, Maechler P and Wollheim CB (1998) Effects of depletion of mitochondrial DNA in metabolism secretion coupling in INS-1 cells. Journal of Inherited Metabolic Disease 47, 374-380

96. Revollo JR, Körner A, Mills KF et al (2007) Nampt/PBEF/visfatin regulates insulin secretion in β cells as a systemic NAD biosynthetic enzyme. Cell metabolism 6, 363-375

97. Vetterli L, Brun T, Giovannoni L, Bosco D and Maechler P (2011) Resveratrol potentiates glucose-stimulated insulin secretion in INS-1E β-cells and human islets through a SIRT1-dependent mechanism. Journal of biological chemistry 286, 6049-6060

98. Potthast AB, Heuer T, Warneke SJ and Das AM (2017) Alterations of sirtuins in mitochondrial cytochrome c-oxidase deficiency. PLoS One 12, e0186517

99. Oh YS, Seo E, Park K and Jun H-S (2017) Compound 19e, a novel glucokinase activator, protects against cytokine-induced beta-cell apoptosis in INS-1 cells. Frontiers in Pharmacology 8, 169